Comparing Backscatter Communication and Energy Harvesting in Massive IoT Networks

Rong Du, Thomas Ohlson Timoudas, *Member, IEEE*, and Carlo Fischione, *Senior Member, IEEE*

***Abstract*— Backscatter communication (BC) and radio-frequency energy harvesting (RF-EH) are two promising technologies for extending the battery lifetime of wireless devices. Although there have been some qualitative comparisons between these two technologies, quantitative comparisons are still lacking, especially for massive IoT networks. In this paper, we address this gap in the research literature, and perform a quantitative comparison between BC and RF-EH in massive IoT networks with multiple primary users and multiple low-power devices acting as secondary users. An essential feature of our model is that it includes the interferences caused by the secondary users to the primary users, and we show that these interferences significantly impact the system performance of massive IoT networks. For the RF-EH model, the power requirements of digital-to-analog and signal amplification are taken into account. We pose and solve a power minimization problem for BC, and we show analytically when BC is better than RF-EH. The results of the numerical simulations illustrate the significant benefits of using BC in terms of saving power and supporting massive IoT, compared to using RF-EH. The results also show that the backscatter coefficients of the BC devices must be individually tunable, in order to guarantee good performance of BC.**

***Index Terms*— Backscatter communication, energy harvesting, Internet of Things, power optimization.**

I. Introduction

THE next generation of wireless communication systems will be able to manage thousands of machine-type communication or internet-of-things (IoT) devices, even inside small geographic areas. Massive IoT devices, such as wireless sensors for long term monitoring, have low requirements on data rates, but instead have very strict requirements on cost and lifetime, due to their limited battery capacity [1]. This places high requirements on IoT network sustainability. In the following, we define a massive IoT network as a wireless network that supports tens or hundreds of massive IoT devices, inside an area of diameter up to a few hundred meters.

One well-known technology for improving the sustainability of such massive IoT networks is based on radio frequency energy harvesting (RF-EH) [2], which is a type of wireless power communication (WPC). RF-EH uses an energy transmitter that sends radio frequency (RF) waves to the low-power IoT devices, which then harvest and store this energy. The stored energy can then be used for information transmission as needed. However, RF-EH suffers high path loss between the transmitter and the IoT devices, which limits the potential harvested energy. One idea for solving this problem, and increasing the power that can be harvested, is to use multiple antennas and energy beamforming to concentrate the transmitted energy [3], [4]. Other ways to solve the problem is by using a distributed antenna system (DAS) [5], or unmanned aerial vehicles (UAVs) as mobile base stations [6], which could have a better coverage performance than a traditional base station with co-located antennas. Interference alignment is used in [7] to add artificial noise that can be harvested for energy, and that can prevent eavesdropping.

Another possible technology for network sustainability is backscatter communication (BC) [8], [9]. Instead of harvesting the RF energy and using it later, an IoT node could act as a backscatter transmitter to modulate the data by switching its antenna impedance state [8], to backscatter the signal from a carrier emitter to the backscatter receiver. Compared to WPC, BC has the following advantages: 1) It does not incur the RF to direct current (RF-DC) conversion losses present in WPC during the energy harvesting (EH) process; 2) A backscatter transmitter does not convert the data to analog signals and does not amplify the signal [10]. Therefore, it does not need digital-to-analog converter (DAC) and power amplifier (PA) circuits, which are the most power consuming components in generic RF transceivers. Thus, BC offers great potential for enabling green and sustainable IoT devices. However, traditional BC systems suffer a major problem: the ambient signal may be too weak, hindering applications of BC in dense networks.

To support the development of BC for green and sustainable massive IoT networks, we must require the carrier emitter to be controllable, to ensure that the signal reaching the backscatter transmitter is strong enough. The carrier emitter should also transmit information to its own destination, instead of purely sending signals for backscattering devices, and network

Manuscript received November 29, 2020; revised March 22, 2021; accepted July 1, 2021. Date of publication July 20, 2021; date of current version January 10, 2022. This work was supported in part by the Digital Futures Project DEMOCRITUS, in part by the Vinnova Project iWater, and in part by the Energimyndigheten and Swedish Research Council Project ADVANCE. The associate editor coordinating the review of this article and approving it for publication was X. Tao. *(Rong Du and Thomas Ohlson Timoudas are co-first authors.) (Corresponding author: Thomas Ohlson Timoudas.)*

Rong Du was with the Network and Systems Engineering Division, Computer Science Department, KTH Royal Institute of Technology, 100 44 Stockholm, Sweden. He is now with Ericsson AB, 164 83 Kista, Sweden (e-mail: rongd@kth.se).

Thomas Ohlson Timoudas is with the Network and Systems Engineering Division, Computer Science Department, KTH Royal Institute of Technology, 100 44 Stockholm, Sweden (e-mail: ttohlson@kth.se).

Carlo Fischione is with the Network and Systems Engineering Division, Computer Science Department, KTH Royal Institute of Technology, 100 44 Stockholm, Sweden (e-mail: carlofi@kth.se).

Color versions of one or more figures in this article are available at https://doi.org/10.1109/TWC.2021.3096800.

Digital Object Identifier 10.1109/TWC.2021.3096800

optimization should be used to improve system performance. Therefore, we consider a system as shown in Fig. 1, which contains a DAS base station, acting as the carrier emitter, that needs to transmit some information to its own intended users, the primary users in the network. At the same time, the base station aims to support the massive IoT devices, which use BC to transmit information to their own respective destinations (BC receivers). The backscatter transmitters and receivers are considered secondary transmitters and secondary receivers in the system. The whole system should ensure that the quality of service (QoS) requirements in terms of data rates are met for all the users, while at the same time minimizing the total power consumed at the base station.

To understand the potential benefits of using the system we consider, we compare it to a similar system, in which the IoT devices, instead of using BC, harvest RF energy from the base station and transmit their data at a later time (we call this (energy)-harvest-then-transmit (HTT) [11], [12] in the following). We are interested in the comparison of the backscatter and the energy harvesting solutions. We summarize our main contributions and novelties as follows:

- We make a quantitative comparison between BC and HTT in a massive IoT network, in the sense that all the parameters for the requirements are the same, with the only difference being the application of either BC or HTT. For each of these technologies, we formulate an optimization problem. We take into account the most important factors that are usually neglected in the literature, such as the interferences caused by backscattering, and the power consumption in digital to analog conversion and signal amplification in HTT technologies, making the system models more accurate and realistic. Our simulations demonstrate that these factors should not be neglected, especially for massive IoT networks.
- The two optimization problems above are difficult to solve in general. For the BC case, we provide a numerical algorithm to achieve the optimal solution, and a closed-form solution for the special case when the base station has a single antenna. For the HTT case, we can establish a performance bound, which allows us to perform numerical comparisons between the two technologies. We also provide analytical results to show that the BC technology outperforms the HTT technology under selected conditions on the hardware parameters.

The algorithm for obtaining the optimal solution for BC in the single-antenna case has appeared in our earlier conference paper [13], for the case of a single primary user. Here, we greatly extend the results in that paper to the cases of multiple primary users, and provide the full proof of these extended results in the Appendix.

The rest of the paper is organized as follows. In Section II, we review related work about BC and WPC. In Section III, we provide the details of the system model and formulate optimization problems for the two technologies. We present our analytical results in Section IV, based on which we perform numerical studies in Section V. We summarize our work in Section VI.

Notation: Bold, non-italic, upper-case Latin characters $(\mathbf{A}, \mathbf{Q})$ denote matrices; bold, italic characters $(\boldsymbol{\alpha}, \boldsymbol{P}^t)$ denote (column) vectors; and regular characters (i, N) represent scalars. Bold numbers $(\mathbf{0}, \mathbf{1})$ denote vectors with all elements equal to the corresponding number. Inequalities involving vectors or matrices $(\boldsymbol{v} \geq \boldsymbol{x})$ are meant element-wise (e.g., for every i, $v_i \geq x_i$). The transpose of a vector/matrix is denoted $\boldsymbol{v}^T$ or $\mathbf{M}^T$, and the conjugate transpose $\mathbf{M}^H$.

II. Related Work

The seminal work [8] presents the design and prototype of an ambient BC system, which allows two devices to communicate by leveraging ambient RF signals from TV or cellular transmissions. The backscatter transmitter uses a switch that modulates the impedance of the antenna between reflective and absorptive states to convey bits to its receiver. This design avoids the process of generating radio waves at the device and therefore uses less power and energy than traditional radio communication. The work in [14] subsequently introduced a multi-antenna design and a coding mechanism based on CDMA to extend the communication range and allow concurrent transmissions. Several different modulation schemes and signal detection algorithms for BC [15]–[17] have been proposed to achieve this same goal. These designs successfully showcase the great potential of using ambient backscatter communication for low-power or battery-less devices.

There are several recent studies that optimize the performance of backscatter communication systems. In [18], the authors have studied a BC system with power domain non-orthogonal multiple access (NOMA) and time division multiple access. The backscatter transmitters can choose their reflection coefficients to make the channel gains of different backscatter transmitters more significant, and the receiver decodes the data from multiple transmitters using successive interference cancellation (SIC). The authors of [19] have investigated a hybrid system where the transmitter can use either BC or WPC to transmit data to its receiver. They have analyzed the outage probability, coverage, and throughput of the system using stochastic geometry. The authors of [20] have formulated a throughput maximization problem for a system that integrates wireless power transfer and BC. Similarly, [21] studies throughput maximization for a time division multiple access scheme, allowing a subset of the devices to backscatter to nearby devices in each time slot. Time switching and power splitting are used in [22] to maximize output capacity, letting each device backscatter only on one channel, and harvest energy from the remaining channels. Outage performance of BC systems is studied in [23] using Monte-Carlo simulations.

Most of the works mentioned above only consider the performance of the backscatter transmitters and their receivers in isolation, ignoring the impact of interference caused by the backscatter devices on the legacy (primary user) receivers of the carrier emitter (or base station). In contrast to these, we also take into account the legacy users in the system, with the aim of ensuring that, even with the interference from the backscatter devices, the throughput requirements of the legacy users are met.

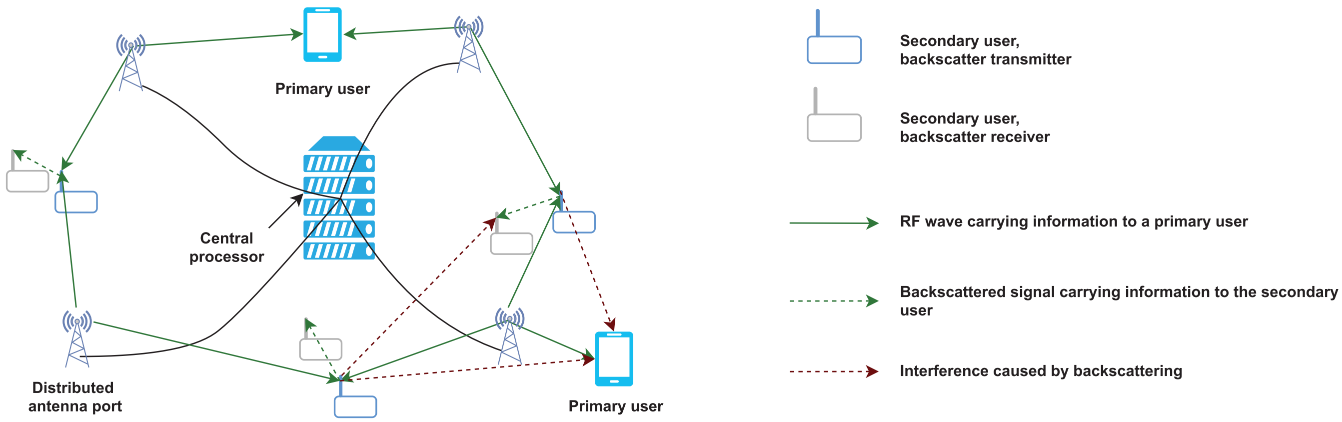

Fig. 1. An illustration of the system considered in this paper. A distributed antenna system is used to transmit information to its primary users, and the wireless signals from the distributed antenna system are in turn leveraged by the massive IoT devices, considered secondary users, to transmit information to their own destination.

One way to handle the interferences caused by the backscattering devices is to apply time scheduling. That is, each backscatter device is assigned a mini slot in which it may backscatter the signal, while the other devices could harvest the energy. Many studies have attempted to optimize such time schedules, see e.g. [24]–[26]. However, the energy harvesting models in these studies are oversimplified. The energy consumption in the power amplifier and DAC are not considered. Thus, the results may be over-optimistic. More importantly, time scheduling schemes do not scale well with the number of backscatter devices. The reason is that, when there are many backscatter devices, a device may only get a very limited time duration for data transmission. Moreover, guard time is needed in practice to avoid interference, making such schemes inefficient. Thus, these solutions may fail in massive IoT networks. In our paper, instead of considering time scheduling, we allow all backscatter devices to backscatter at the same time, taking the interference into account, while carefully optimizing the power of the base station and the backscatter coefficients of the backscatter devices, to ensure that the QoS requirements are met.

III. System Models and Formulation of the Problems

We consider a massive IoT network, consisting of one base station serving M primary users, and N secondary user pairs (a transmitter paired with a receiver). The transmitter of each secondary user pair is a low-power IoT device that needs to send data to its corresponding receiver, such as a gateway, which has greater computing and power capacity. The secondary users are interested in taking advantage of the "ambient" energy of the RF signals carrying information to the primary users, not their content, using either BC or HTT (we consider both cases in this paper), which is why the network serves them only when the QoS of the primary users can be guaranteed while doing so. We assume that both the primary and secondary users have only one antenna (see also [19], [25], [27]). We make this assumption to simplify the model, and because of the low-power setting. The case of multiple receiver antennas is an interesting problem that could be considered in a future work. The base station has a CP (central processor) and K antenna ports, each of which has one antenna, as shown in Fig. 1. The CP maintains the channel state information, makes decisions, and processes baseband signals. The ports are used for RF signal operations, and are located in different places in the area and connect to the CP using high capacity backhaul links.

The channels are modeled as frequency-flat and quasi-static. We consider a scenario where the base station sends downlink multicast messages to the primary users in a frame with normalized duration $T = 1$. The received signal of the primary user m is then $y_{\mathrm{p},m} = \boldsymbol{h}_{\mathrm{p},m}^H \boldsymbol{x} + n_{\mathrm{p},m}$, where $\boldsymbol{h}_{\mathrm{p},m} = [h_{1,\mathrm{p},m}, h_{2,\mathrm{p},m}, \ldots, h_{K,\mathrm{p},m}]^H$ is the channel coefficient vector between the ports and the primary user, $\boldsymbol{x}$ is the transmitted signal to the primary user, and $n_{\mathrm{p},m}$ is additive white Gaussian noise with zero mean and variance σ^2. Let $\mathbf{Q}_{\mathrm{p}} = \mathbb{E}[\boldsymbol{x}\boldsymbol{x}^T]$ denote the covariance of Gaussian input, and recall that the distributed ports have independent power budgets. Thus, they do not code and process the signal jointly, meaning that the signals at the ports are independent. Therefore, $\mathbf{Q}_{\mathrm{p}} = \mathrm{diag}\{p_1, p_2, \ldots, p_k\}$, where p_i is the transmit power of port i. This formulation is similar to the one in [5].

Whenever the base station transmits information to the primary users (PUs), the RF signals also reach the secondary users (SUs). These signals can then be used by the secondary users for their own transmission purposes, as long as they do not cause significant interference to the primary users. One possible way of doing this is using BC, and another one is using HTT. We will separately discuss these two technologies in more detail in the following subsections. Lastly, we denote the source and destination of the i-th secondary user pair by SU-TX i and SU-RX i, respectively. The channel gain from SU-TX i to SU-RX j is denoted g_{ij}, and $\boldsymbol{h}_i = [h_{1,i}, \ldots, h_{K,i}]^T$ represents the channel coefficient vector between the antenna ports and SU-TX i. Similarly, $g_{i,\mathrm{p},m}$ denotes the channel gain from SU-TX i to primary user m.

A. Secondary Users Applying Backscatter Communication

In this case, each SU-TX applies BC to transmit data to its respective destination, or SU-RX. More specifically, each

SU-TX backscatters the signal from the base station to its destination by changing the impedance of its antenna. The energy required to do so is negligible and does not require the use of a DAC or PA circuit. On the receiver side, each SU-RX i receives the combined signals of the following: 1) the signal carrying information to the PU; 2) the signal carrying information from SU-TX i; 3) the signals carrying information from the other SU-TXs; and 4) noise. In a typical backscatter communication system, the signal carrying information to the PU is not seen as interference, using filter approaches such as envelope detectors [8], [14]. Therefore, the signal-to-noise-and-interference-ratio (SINR) at SU-RX i is $\text{SINR}_{i,\text{BC}} = (\alpha_i g_{ii} \boldsymbol{h}_i^H \mathbf{Q}_\text{p} \boldsymbol{h}_i)/(\sigma^2 + \sum_{j\neq i} \alpha_j g_{ji} \boldsymbol{h}_j^H \mathbf{Q}_\text{p} \boldsymbol{h}_j)$, which can be simplified as $\text{SINR}_{i,\text{BC}} = (\alpha_i g_{ii} \sum_{k=1}^K p_k |h_{k,i}|^2)/(\sigma^2 + \sum_{j\neq i} \alpha_j g_{ji} \sum_{k=1}^K p_k |h_{k,j}|^2)$, where $\alpha_i \in [0, \alpha_{\max}]$ is the backscatter coefficient that corresponds to the ratio of the source signal power that is backscattered by SU-TX i, and $\alpha_{\max} < 1$ is the maximum backscatter coefficient. The data rate of BC depends on the frequency of switching the states of the impedance, and is assumed to be pre-determined here. Therefore, any given data rate requirement can be translated into an SINR requirement at the receiver. Namely, the SINR must exceed some threshold, denoted by γ_BC, which depends on the desired data rate.

Since the backscattered signals interfere with the primary users, the SINR of the primary user m is $\text{SINR}_{\text{p},m,\text{BC}} = (\sum_{k=1}^K p_k |h_{k,\text{p},m}|^2)/(\sigma^2 + \sum_{i=1}^N \alpha_i g_{i,\text{p},m} \sum_{k=1}^K p_k |h_{k,i}|^2)$, where $g_{i,\text{p},m}$ is the channel gain from SU-TX i to the primary user m. The primary users have a QoS requirement that their downlink data rate must exceed a pre-determined threshold R_p. This requirement can be formulated as $W \log_2 (1+\text{SINR}_{\text{p},m,\text{BC}}) \geq R_\text{p}$, for every m, where W is the bandwidth. Denote the power of the K antenna ports by $\boldsymbol{p} = [p_1, \ldots, p_K]^T$, and set $\boldsymbol{\alpha} = [\alpha_1, \ldots, \alpha_N]^T$. This constraint is then equivalent to $\text{SINR}_{\text{p},m,\text{BC}} \geq \gamma_\text{p}$, for every m, with $\gamma_\text{p} = 2^{R_\text{p}/W} - 1$. When the secondary users apply BC, we can formulate the power allocation problem as follows:

$$\min_{\boldsymbol{p},\boldsymbol{\alpha}} \sum_{k=1}^K p_k \tag{1a}$$

$$\text{s.t.} \quad \frac{\sum_{k=1}^K p_k |h_{k,\text{p},m}|^2}{\sigma^2 + \sum_{i=1}^N \alpha_i g_{i,\text{p},m} \sum_{k=1}^K p_k |h_{k,i}|^2} \geq \gamma_\text{p}\,, \quad m = 1, \ldots, M\,, \tag{1b}$$

$$\frac{\alpha_i g_{ii} \sum_{k=1}^K p_k |h_{k,i}|^2}{\sigma^2 + \sum_{j\neq i} \alpha_j g_{ji} \sum_{k=1}^K p_k |h_{k,j}|^2} \geq \gamma_\text{BC}\,, \quad i = 1, \ldots, N, \tag{1c}$$

$$0 \leq p_k \leq P\,, k = 1, \ldots, K, \tag{1d}$$

$$0 \leq \alpha_i \leq \alpha_{\max}\,, i = 1, \ldots, N. \tag{1e}$$

The objective is to minimize the total power (for the sake of energy efficiency), with the Constraint (1b) representing the QoS requirement of the primary users, (1c) representing the SINR requirement for the SU-RXs, and (1d) representing the maximum power that each antenna port can use. Problem (1) is non-convex due to the multiplication of the variables α and p. Note that Problem (1) ensures that the QoS requirements for all PUs and SUs are met, as long as the SUs use the $\boldsymbol{\alpha}$ computed by the base station. If some SUs are malicious, i.e., they do not follow the decision and want to cause large interference, then the base station could try to mitigate by removing Constraints (1c) for the malicious SUs and replacing α_i of the malicious SUs by $\alpha_{\max}$.

B. Secondary Users Applying Harvest-Then-Transmit

We now consider the second case, in which the SU-TXs first harvest the RF energy from the BS, and then transmit data to their corresponding receivers, instead of using BC.

We first consider the SU-TXs. For SU-TX i, the received power from the ports is $P_i^\text{r} = \boldsymbol{h}_i^H \mathbf{Q}_\text{p} \boldsymbol{h}_i = \sum_k p_k |h_{k,p}|^2$. The harvested power is $P_i^\text{h} = \eta_\text{RF-DC}(P_i^\text{r})$, where $\eta_\text{RF-DC}(\cdot)$ is the RF-DC conversion function. In general, $\eta_\text{RF-DC}(\cdot)$ is a nonlinear function due to the diode non-linearity and the saturation behaviour [6]. However, in the literature [27]–[29], it is common to assume that it is linear, for the sake of analytical simplicity. As we will see later on in this paper, the problem is difficult to solve even when $\eta_\text{RF-DC}(\cdot)$ is assumed to be linear. Therefore, we use a linear model, i.e., $P_i^\text{r} = \eta P_i^\text{r}$, and set η as the maximum gradient of $\eta_\text{RF-DC}(\cdot)$, which guarantees that the harvested energy is never under-estimated. We will later show that even using this over-optimistic, or over-estimated, model results in worse performance than using BC.

Recall that the duration of the time frame is normalized to be 1. If SU-TX i harvests energy for the duration $t_i \leq 1$, then the total energy it harvests is $\eta t_i P_i^\text{r}$. In the remaining time $1 - t_i$, SU-TX i transmits its data to its corresponding destination with power P_i^t. We assume that $1 - t_i \geq t_{\min}$, which corresponds to the minimum transmission time of the transceiver. Then, the requirement that the amount of consumed energy must not exceed the amount of harvested energy gives us the constraint $(1 - t_i)(P_i^\text{t}/\eta_\text{PA} + P^\text{DAC}) \leq \eta t_i \boldsymbol{h}_i^H \mathbf{Q}_\text{p} \boldsymbol{h}_i$ [30]. Here, $\eta_\text{PA} < 1$ is the power amplifier efficiency (different from the power amplifier gain), and P^DAC is the power usage of the power amplifier, which are ignored in most of the related studies, and results in an over-simplified model and an over-optimistic performance. For the sake of fairness, we assume that the SU-RX also in the HTT case does not see the signal to the primary users as interference (for instance, by using different frequency bands). Then, the SINR at SU-RX i is [18] $\text{SINR}_{i,\text{EH}} = g_{ii} P_i^\text{t}/(\sigma^2 + \sum_{j\neq i} g_{ji} P_j^\text{t})$. Thus, the maximum amount of data SU-TX i can send to its receiver is $(1 - t_i) W \log_2(1 + \text{SINR}_{i,\text{EH}})$.

Regarding the primary users, the SINR of the primary user m is

$$\text{SINR}_{\text{p},m,\text{EH}} = \frac{\boldsymbol{h}_{\text{p},m}^H \mathbf{Q}_\text{p} \boldsymbol{h}_{\text{p},m}}{\sigma^2 + \sum_{i=1}^N g_{i,\text{p},m} P_i^\text{t}} = \frac{\sum_{k=1}^K p_k |h_{k,\text{p},m}|^2}{\sigma^2 + \sum_{i=1}^N g_{i,\text{p},m} P_i^\text{t}}.$$

Let $\boldsymbol{P}^\text{t} = [P_1^\text{t}, \ldots, P_N^\text{t}]^T$ and $\boldsymbol{t} = [t_1, \ldots, t_N]^T$. Then, similar to Problem (1), we can formulate the power allocation problem for the HTT case as follows:

$$\min_{\boldsymbol{p},\boldsymbol{t},\boldsymbol{P}^\text{t}} \sum_{k=1}^K p_k \tag{2a}$$

$$\text{s.t.} \quad \frac{\sum_{k=1}^K p_k |h_{k,\text{p},m}|^2}{\sigma^2 + \sum_{i=1}^N g_{i,\text{p},m} P_i^\text{t}} \geq \gamma_\text{p}, m = 1, \ldots, M\,, \tag{2b}$$

$$(1-t_i)W\log_2\left(1+\frac{g_{ii}P_i^{\mathrm{t}}}{\sigma^2+\sum_{j\neq i}g_{ji}P_j^{\mathrm{t}}}\right)\geq R_{\mathrm{s}}\,,\quad i=1,\dots,N, \tag{2c}$$

$$(1-t_i)\left(\frac{P_i^{\mathrm{t}}}{\eta_{\mathrm{PA}}}+P^{\mathrm{DAC}}\right)\leq \eta t_i\boldsymbol{h}_i^H\mathbf{Q}_{\mathrm{p}}\boldsymbol{h}_i\,,\quad i=1,\dots,N, \tag{2d}$$

$$0\leq t_i\leq 1-t_{\min}\,, i=1,\dots,N, \tag{2e}$$

$$0\leq p_k\leq P\,, k=1,\dots,K, \tag{2f}$$

$$0\leq P_i^{\mathrm{t}}\,, i=1\dots,N. \tag{2g}$$

For the sake of fairness, the required data rate of the SU-RXs is the same as in the case for BC, i.e., $R_{\mathrm{s}}=W\log_2(1+\gamma_{\mathrm{BC}})$. Problem (2) is also non-convex, due to the multiplication of the decision variables (e.g., in Constraint (2d)).

C. Problem Formulation

We are now in a position to present the problem we are interested in, in this paper, as follows: Given the QoS and rate requirements of the primary user and the SU-RXs, which technology is more energy-efficient: BC or HTT? To answer this question, we would have to solve Problem (1) and Problem (2), and compare their two optima. However, these optima depend on the parameters, such as $\alpha_{\max}$, η, $t_{\min}$. Since both of these problems are non-convex, they are not trivial to solve, and therefore an analytical comparison between BC and HTT is non-trivial.

IV. Theoretical Results

In this section, we first present our solution to the backscatter problem, and then compare BC and HTT. Since the HTT problem (2) is difficult to solve, we start with a special case, in which it is possible to compare the optimal solutions to the two problems (1) and (2) without solving them. For the general cases, we compare BC and HTT by analyzing performance bounds of the optimal HTT solution. For the sake of fairness, we will assume that the parameters W, R_{p}, R_{s} (equivalently γ_{BC}), P, and the channel gains are the same for the two problems.

A. Solution in the Backscatter Communication Case

Although Problem (1) is non-convex, we can transform it to a linear optimization problem by using an auxiliary variable $P_{i,\mathrm{BC}}^{\mathrm{t}}=\alpha_i\sum_{k=1}^K p_k|h_{k,i}|^2$ as follows. Then, the requirement that $\alpha_i\leq\alpha_{\max}$ is equivalent to $P_{i,\mathrm{BC}}^{\mathrm{t}}\leq\alpha_{\max}\sum_{k=1}^K p_k|h_{k,i}|^2$. Problem (1) then becomes

$$\min_{\boldsymbol{p},\boldsymbol{P}_{\mathrm{BC}}^{\mathrm{t}}}\ \sum_{k=1}^K p_k \tag{3a}$$

$$\text{s.t.}\ \frac{\sum_{k=1}^K p_k|h_{k,\mathrm{p},m}|^2}{\sigma^2+\sum_{i=1}^N g_{i,\mathrm{p},m}P_{i,\mathrm{BC}}^{\mathrm{t}}}\geq\gamma_{\mathrm{p}}, m=1,\dots,M, \tag{3b}$$

$$\frac{g_{ii}P_{i,\mathrm{BC}}^{\mathrm{t}}}{\sigma^2+\sum_{j\neq i}g_{ji}P_{j,\mathrm{BC}}^{\mathrm{t}}}\geq\gamma_{\mathrm{BC}}, i=1,\dots,N\,, \tag{3c}$$

$$0\leq p_k\leq P, k=1,\dots,K\,, \tag{3d}$$

$$0\leq P_{i,\mathrm{BC}}^{\mathrm{t}}\leq\alpha_{\max}\sum_{k=1}^K p_k|h_{k,i}|^2, i=1,\dots,N. \tag{3e}$$

Algorithm 1 Solution for Problem (1)

Input: Parameters of Problem (1)
Output: Optimal solution $\boldsymbol{p}^*,\boldsymbol{\alpha}^*$
1: Construct Problem (3) according to Problem (1)
2: **if** Problem (3) is feasible **then**
3: Achieve optimal solution $(\boldsymbol{p}^*,\boldsymbol{P}_{\mathrm{BC}}^{\mathrm{t},*})$ of Problem (3) with linear programming
4: $\alpha_i^*\leftarrow P_{i,\mathrm{BC}}^{\mathrm{t},*}/\sum_{k=1}^K p_k^*|h_{k,i}|^2$ for all i
5: **return** $(\boldsymbol{p}^*,\boldsymbol{\alpha}^*)$
6: **else**
7: **return** No feasible solution
8: **end if**

We show that Problem (3) is a linear optimization one, as summarized by the following theorem:

Theorem 1: Problem (3) *is a linear optimization problem.*

Proof: The objective function of Problem (3), and the Constraints (3d) and (3e), are linear functions. What remains is to show that Constraints (3b) and (3c) are equivalent to linear constraints. Since the channel gains from SU-TX i to the primary users ($g_{i,\mathrm{p},m}$) and SU-RX i ($g_{i,j}$) are positive, we can multiply the denominator of Constraints (3b) and (3c) to the right-hand side and the resulting constraints are linear, which completes the proof. ■

Based on Theorem 1, we can easily solve Problem (3). Denote its optimal solution by $(\boldsymbol{p}^*,\boldsymbol{P}_{\mathrm{BC}}^{\mathrm{t},*})$. Then, we can obtain the optimal solution to Problem (1) as $(\boldsymbol{p}^*,\boldsymbol{\alpha}^*)$, where $\alpha_i^*=P_{i,\mathrm{BC}}^{\mathrm{t},*}/\sum_{k=1}^K p_k^*|h_{k,i}|^2$, as summarized in Algorithm 1. Note that Algorithm 1 has the same complexity as solving a linear program.

Proposition 1: The complexity of Algorithm 1 is the same as the complexity of solving a linear program. Using an interior point method, the complexity is no higher than $O(n^3L)$ or $O(\frac{n^3}{\log n}L)$ [31], with L equal to the bit length of the input data, and $n=\max(K,N,M)$.

In addition to Algorithm 1, we also develop a closed-form solution to Problem (1) in a special case, that we will present in the next subsection.

B. Closed-Form Solution in the Backscatter Communication Case With a Single-Antenna Base Station

In this subsection, we still focus on the BC technology, and we will restrict to the case of one antenna, that is $K=1$. We will therefore suppress the indices k corresponding to the antenna ports. Since it is possible to obtain a simple closed-form solution in this special case, it is of particular interest. The material in this subsection is an extension of our earlier conference paper [13], with the major addition that here we consider the case of multiple primary users.

First, we will reformulate Problem (1), and then give a closed-form solution to the problem. Notice that the inequalities in (1c) can be equivalently stated as

$p|h_{\mathrm{p},m}|^2 - \gamma_{\mathrm{p}} \sum_{i=1}^{N} \alpha_i g_{i,\mathrm{p},m} p|h_i|^2 \geq \sigma^2\gamma_{\mathrm{p}}$ (when $K = 1$), after rearranging them. This can be further simplified as $\mathbf{S}p\boldsymbol{\alpha} \geq \mathbf{1}$, by introducing the $N \times N$ matrix

$$\mathbf{S} \triangleq (w_{ij}), \tag{4}$$

with $w_{ii} = g_{ii}|h_i|^2/(\sigma^2\gamma_{\mathrm{BC}})$, and $w_{ij} = -g_{ji}|h_j|^2/\sigma^2$ if $i \neq j$. Since each g_{ji} denotes the channel gain from SU-TX j to SU-RX i, and is thus strictly positive, the diagonal elements of $\mathbf{S}$ are all strictly positive, and the off-diagonal ones strictly negative.

Next, introduce the real-valued functions B_m on $\mathbb{R}^N$, for $1 \leq m \leq M$, given by

$$B_m(\boldsymbol{v}) \triangleq b_{m0} + \sum_{i=1}^{N} b_{mi} v_i, \tag{5}$$

with $b_{m0} = |h_{\mathrm{p},m}|^2/(\sigma^2\gamma_{\mathrm{p}})$, and $b_{mi} = -g_{i,\mathrm{p},m}|h_i|^2/\sigma^2$ when $1 \leq i \leq N$. Just like above, the inequalities in (1c) can be rearranged and expressed (when $K = 1$) as

$$\alpha_i g_{ii} p|h_i|^2 - \gamma_{\mathrm{BC}} \sum_{j \neq i} \alpha_j g_{ji} p|h_j|^2 \geq \sigma^2\gamma_{\mathrm{BC}},$$

which can be further simplified as $pB_m(\boldsymbol{\alpha}) \geq 1$ for every $1 \leq m \leq M$. Given a vector $\boldsymbol{v} > \mathbf{0}$, each of the functions $\mathbb{R} \ni t \mapsto B_m(t\boldsymbol{v})$ is monotone decreasing, since every b_{mi} is strictly negative for $1 \leq i \leq N$. Since $b_{m0} > 0$, it follows that $B_m(\mathbf{0}) > 0$. These properties will play an important role later on in the proofs in the Appendix.

If we ignore the upper bound $p \leq P$, then Problem (1) is equivalent to the following problem when $K = 1$:

$$\min_{p,\boldsymbol{\alpha}} \ p \tag{6a}$$
$$\text{s.t. } pB_m(\boldsymbol{\alpha}) \geq 1, m = 1, \ldots, M \tag{6b}$$
$$\mathbf{S}p\boldsymbol{\alpha} \geq \mathbf{1}, \tag{6c}$$
$$0 \leq p, \text{ and} \tag{6d}$$
$$\mathbf{0} \leq \boldsymbol{\alpha} \leq \alpha_{\max}\mathbf{1}. \tag{6e}$$

That is, an optimal solution $(p^*, \boldsymbol{\alpha}^*)$ to Problem (6) is also an optimal solution to Problem (1), if and only if $p^* \leq P$. We have the following feasibility result.

Theorem 2: The following condition is necessary and sufficient for Problem (6) *to be feasible*:

- *The equation $\mathbf{S}\boldsymbol{v} = \mathbf{1}$ has a positive solution $\boldsymbol{v} > \mathbf{0}$.*

The proof can be found in the Appendix, where it is also shown that the solution $\boldsymbol{v}$ must be unique, if it exists. Our next result shows how such a solution can be directly used to compute the optimal solution $(p^*, \boldsymbol{\alpha}^*)$ to Problem (6), and to solve our original problem, Problem (1).

Theorem 3: Suppose that Problem (6) *is feasible. Then it has a unique optimal solution $(p^*, \boldsymbol{\alpha}^*)$ that satisfies*

$$(p^*, \boldsymbol{\alpha}^*) = (\frac{1}{t}, t\boldsymbol{v}),$$

where $\boldsymbol{v} > 0$ is the (unique) solution to $\mathbf{S}\boldsymbol{v} = \mathbf{1}$, and

$$t = \min\left\{\frac{\alpha_{\max}}{\|\boldsymbol{v}\|_\infty}, \min_{1 \leq m \leq M}\left\{\frac{b_{m0}}{1 - \sum_{i=1}^{N} b_{mi} v_i}\right\}\right\}.$$

Algorithm 2 Backscatter Coefficient Balancing (BCB)

Input: Parameters of Problem (1) for $K = 1$.
Output: Optimal solution $\boldsymbol{p}^*, \boldsymbol{\alpha}^*$ to Problem (1) when $K = 1$.

1: Initialize w_{ij} and $\mathbf{S}$ in (4), and b_{ij} and B_m in (5).
2: Find $\boldsymbol{v}$ that satisfies $\mathbf{S}\boldsymbol{v} = \mathbf{1}$.
3: **if** such $\boldsymbol{v}$ exists, and $\min_{0 \leq i \leq N} v_i > 0$ **then**
4:    $t \leftarrow \min\left\{\alpha_{\max}/\|\boldsymbol{v}\|_\infty, \min_{1 \leq m \leq M}\left\{b_{m0}/(1 - \sum_{i=1}^{N} b_{mi} v_i)\right\}\right\}$
5:    $p^* \leftarrow 1/t$
6:    $\boldsymbol{\alpha}^* \leftarrow t\boldsymbol{v}$
7:    **if** $p^* \leq P$ **then**
8:      **return** The optimal solution is $(\boldsymbol{\alpha}^*, p^*)$.
9:    **end if**
10: **else**
11:    **return** The problem has no solution.
12: **end if**

In particular, when $K = 1$, Problem (1) *has an optimal solution, if and only if Problem* (6) *is feasible and $p^* \leq P$, which is then unique and equal to $(p^*, \boldsymbol{\alpha}^*)$.*

Using these results, we formulate a solution algorithm (Algorithm 2). It takes as input the parameters of the problem, recalling that the number of antennas is $K = 1$, and returns the unique optimal solution to Problem (1), if it exists. As can be seen on Lines 2 and 3, the algorithm first checks if the basic feasibility condition for Problem (6) in Theorem 2 is satisfied. It then computes the optimal solution for Problem (6), following the results in Theorem 3. On Line 7, the final condition for feasibility of Problem (1) is checked. In the final step, the algorithm returns the optimal solution, if it exists. It is evident that:

Proposition 2: The complexity of Algorithm 2 is the same as the complexity of solving a linear system of N equations with N unknowns, which is no worse than $O(N^3)$.

We have now shown how to obtain the optimal solution for the backscatter communication case. Unfortunately, it is not easy to find the optimal solution to the HTT case. Therefore, in the next subsection, we will compare the optima of the two technologies without solving them.

C. Comparison Between BC and HTT in a Special Case

We study a special case in which $\alpha_{\max} \geq \eta\eta_{\mathrm{PA}}$, and recall that η and η_{PA} are the efficiency of EH and the efficiency of PA, respectively. This special case is actually highly relevant, since $\alpha_{\max} \geq \eta\eta_{\mathrm{PA}}$ typically holds in many practical cases: For BC, some typical values of $\alpha_{\max}$ used in the literature are relatively large, e.g., 0.81 in [32], 0.7 in [18], and 0.6 in [25]. The energy harvesting rate η is usually not high, e.g. 0.15 in [10], 0.4 in [33], and less than 0.4 in [34]. The PA efficiency η_{PA} is around 0.7 [30]. In this special case, we have the following result:

Theorem 4: Consider Problem (1) *and Problem* (2) *with the same problem inputs R_p, γ_{BC}, P, and channel gains. If Problem* (2) *is feasible, then Problem* (1) *is also feasible. Suppose that they are both feasible, and let p^*_{BC} and p^*_{EH} be* *the optimum of Problem* (1) *and Problem* (2)*, respectively. If $\alpha_{\max} \geq \eta\eta_{PA}$, then $p^*_{BC} \leq p^*_{EH}$, i.e., BC always outperforms HTT.*

Proof: Recall that Problem (1) is equivalent to Problem (3). The idea of this proof is to show that all feasible points for Problem (2) are feasible for Problem (3), and thus for Problem (1). More precisely, we will show that, given a feasible solution $(\boldsymbol{p}_{\mathrm{EH}}, \boldsymbol{P}^{\mathrm{t}}_{\mathrm{EH}}, \boldsymbol{t}_{\mathrm{EH}})$ for Problem (2), we can construct a feasible solution $(\boldsymbol{p}_{\mathrm{BC}}, \boldsymbol{P}^{\mathrm{t}}_{\mathrm{BC}})$ for Problem (3) such that $\sum_{k=1}^{K} p_{k,\mathrm{EH}} = \sum_{k=1}^{K} p_{k,\mathrm{BC}}$.

We construct $P^{\mathrm{t}}_{i,\mathrm{BC}} = (1 - t_{i,\mathrm{EH}})P^{\mathrm{t}}_{i,\mathrm{EH}}, \forall i$ and $p_{k,\mathrm{BC}} = p_{k,\mathrm{EH}}, \forall k$. Obviously, $\sum_{k=1}^{K} p_{k,\mathrm{EH}} = \sum_{k=1}^{K} p_{k,\mathrm{BC}}$. The remaining is to show that such a $(\boldsymbol{p}_{\mathrm{BC}}, \boldsymbol{P}^{\mathrm{t}}_{\mathrm{BC}})$ is a feasible solution for Problem (3). We prove it in the following.

From Constraint (2d), we have that $(1 - t_{i,\mathrm{EH}})\left(P^{\mathrm{t}}_{i,\mathrm{EH}}/\eta_{\mathrm{PA}} + P^{\mathrm{DAC}}\right) \leq \eta t_{i,\mathrm{EH}} \sum_{k=1}^{K} p_{k,\mathrm{EH}}|h_{k,i}|^2$, Thus, we have that $(1 - t_{i,\mathrm{EH}})P^{\mathrm{t}}_{i,\mathrm{EH}}/\eta_{\mathrm{PA}} < \eta \sum_{k=1}^{K} p_{k,\mathrm{EH}}|h_{k,i}|^2$. Then we have that $P^{\mathrm{t}}_{i,\mathrm{BC}} < \eta\eta_{\mathrm{PA}} \sum_{k=1}^{K} p_{k,\mathrm{BC}}|h_{k,i}|^2 \leq \alpha_{\max} \sum_{k=1}^{K} p_{k,\mathrm{BC}}|h_{k,i}|^2$, i.e., $(\boldsymbol{p}_{\mathrm{BC}}, \boldsymbol{P}^{\mathrm{t}}_{\mathrm{BC}})$ satisfies Constraint (3e).

Recall that $R_{\mathrm{s}} = W\log_2(1 + \gamma_{\mathrm{BC}})$. Thus, we can show that $(\boldsymbol{p}_{\mathrm{BC}}, \boldsymbol{P}^{\mathrm{t}}_{\mathrm{BC}})$ satisfies Constraint (3c) by proving that

$$W\log_2\left(1 + \frac{g_{ii}P^{\mathrm{t}}_{i,\mathrm{BC}}}{\sigma^2 + \sum_{j\neq i} g_{ji}P^{\mathrm{t}}_{j,\mathrm{BC}}}\right) \geq R_{\mathrm{s}}\,. \tag{7}$$

To prove (7), we define the function $F_i(x) \triangleq W\log_2\left(1 + x/(\sigma^2 + \sum_{j\neq i} g_{ji}P^{\mathrm{t}}_{j,\mathrm{EH}})\right)$ on the domain $x \in [0, +\infty)$. We can see that $F_i(x)$ is concave, and so Jensen's inequality applies to show that $(1 - t_{i,\mathrm{EH}})F_i(P^{\mathrm{t}}_{i,\mathrm{EH}}) + t_{i,\mathrm{EH}}F_i(0) \leq F_i((1 - t_{i,\mathrm{EH}})P^{\mathrm{t}}_{i,\mathrm{EH}})$. Notice that $F_i(0) = 0$, and recall that $(1 - t_{i,\mathrm{EH}})P^{\mathrm{t}}_{i,\mathrm{EH}} = P^{\mathrm{t}}_{i,\mathrm{BC}}$. Thus, Constraint (2c) gives us that

$$R_{\mathrm{s}} \leq (1 - t_{i,\mathrm{EH}})F_i(P^{\mathrm{t}}_{i,\mathrm{EH}}) \leq F_i(P^{\mathrm{t}}_{i,\mathrm{BC}})\,. \tag{8}$$

Since $P^{\mathrm{t}}_{j,\mathrm{BC}} \leq P^{\mathrm{t}}_{j,\mathrm{EH}}$, we have that

$$F_i(P^{\mathrm{t}}_{i,\mathrm{BC}}) \leq W\log_2\left(1 + \frac{P^{\mathrm{t}}_{i,\mathrm{BC}}}{\sigma^2 + \sum_{j\neq i} g_{ji}P^{\mathrm{t}}_{j,\mathrm{BC}}}\right)\,. \tag{9}$$

From (8) and (9), we have that (7) holds. Thus, $(\boldsymbol{p}_{\mathrm{BC}}, \boldsymbol{P}^{\mathrm{t}}_{\mathrm{BC}})$ satisfies Constraint (3c). Similar to the statement to prove (9), we can see that as long as $(\boldsymbol{p}_{\mathrm{EH}}, \boldsymbol{P}^{\mathrm{t}}_{\mathrm{EH}}, \boldsymbol{t}_{\mathrm{EH}})$ satisfies Constraint (2b), $(\boldsymbol{p}_{\mathrm{BC}}, \boldsymbol{P}^{\mathrm{t}}_{\mathrm{BC}})$ satisfies Constraint (3b). It is also straightforward to see that $(\boldsymbol{p}_{\mathrm{BC}}, \boldsymbol{P}^{\mathrm{t}}_{\mathrm{BC}})$ satisfies Constraints (3d) and (3e). To summarize, $(\boldsymbol{p}_{\mathrm{BC}}, \boldsymbol{P}^{\mathrm{t}}_{\mathrm{BC}})$ is a feasible solution for Problem (3), and it holds that $\sum_{k=1}^{K} p_{k,\mathrm{EH}} = \sum_{k=1}^{K} p_{k,\mathrm{BC}}$, which completes the proof. ■

Remark 1: Equality between p^*_{BC} and p^*_{EH} in Theorem 4 holds only when $R_p = 0$ and $\gamma_{BC} = 0$ (i.e., $p^*_{BC} = 0$), which is trivial. For the other cases, strict inequality $p^*_{BC} < p^*_{EH}$ holds, when $\alpha_{\max} \geq \eta\eta_{PA}$.

Remark 2: We can now claim that BC is better than HTT when $\alpha_{\max} \geq \eta\eta_{PA}$, and more importantly, when the backscatter coefficients of the SU-TXs are tunable. If they are not, this theoretical solution may not be achievable even when the condition is satisfied. However, the simulations show that the performance of BC can still be better than HTT even if α is not tunable, due to the non-negligible power usage of the DAC used in HTT.

Although we could not find the optimal solution for the HTT case, we can obtain a performance bound for the HTT case and compare it with the optimum for the BC case in the simulations to gain more insight. In the following subsection, we analyze the bounds for Problems (1) and (2).

D. Performance Bounds

We will first present an upper bound and a lower bound of Problem (1), which will be used in the simulation section for a deeper study.

The upper bound corresponds to the cases where the backscatter coefficients α_i at the SU-TXs are predefined, and the CP is not able to control the backscatter coefficients of the SU-TXs. For the case when the backscatter coefficients α_i are set to be $\alpha_{\max}$ for all the SU-TXs, it means that they all want to greedily backscatter as much power as possible. This gives us an easy way to achieve an upper bound of the optimum of Problem (1), as described in the following:

Proposition 3: Consider a feasible Problem (1)*. Let p^*_{BC} be its optimum, and let $p_{BC}(\alpha_{\max})$ be the optimum of Problem* (1) *given $\alpha_i = \alpha_{\max}$. Then, p^*_{BC} is upper bounded by $p_{BC}(\alpha_{\max})$.*

Remark 3: We call a scheme where all the backscatter coefficients are set to $\alpha_i = \alpha_{\max}, \forall i$ greedy backscatter. *We will use this scheme in the simulations as the upper-bound of the optimum of the backscatter scheme.*

The lower bound corresponds to the cases where the interference caused by the backscattered signals are ignored and are set to be 0. We will refer to this case as the over-optimistic scheme in the simulations, and compare it to the case when the interference is taken into account, to see whether it is important to consider the interference.

Next, we will study the lower bound of the optimum for Problem (2). Before we provide its lower bound, we need to formulate the following optimization problem:

$$\min_{\boldsymbol{p},\boldsymbol{P}^{\mathrm{t}}} \quad \sum_{k=1}^{K} p_k \tag{10a}$$

$$\text{s.t. } W\log_2\left(1 + \frac{g_{ii}P^{\mathrm{t}}_i}{\sigma^2 + \sum_{j\neq i} gn_{ji}P^{\mathrm{t}}_j}\right) \geq R_{\mathrm{s}}\,, \quad i = 1, \ldots, N, \tag{10b}$$

$$\frac{P^{\mathrm{t}}_i}{\eta_{\mathrm{PA}}} + t_{\min}P^{\mathrm{DAC}} \leq \eta \sum_{k=1}^{K} p_k|h_{k,i}|^2\,, \quad i = 1, \ldots, N, \tag{10c}$$

$$\text{(2b), (2f), (2g)}\,.$$

Remark 4: Problem (10) *can be interpreted as follows: Each SU-TX can harvest energy from the base station and transmit information at the same time. This allows us to omit the time variables. We call such a scheme energy harvesting with separated antennas. Problem* (10) *can be transformed, by simple algebraic manipulations, into a linear optimization* *problem. It is therefore easy to obtain the optimal solution to this problem.*

Then, we have the following results:

Proposition 4: Suppose that Problem (2) is feasible. Let p^*_{EH} be its optimum, and let $p^*_{\text{EH,l}}$ be the optimum of the corresponding Problem (10). Then, $p^*_{\text{EH}} \geq p^*_{\text{EH,l}}$.

The proof of Proposition 4 is similar to the one of Theorem 4, and we therefore omit the proof here. Based on this proposition, in the simulations we will solve Problem (10) using the convex optimization solver SeDuMi [35], which is a Matlab toolbox for solving optimization problems such as linear optimization, quadratic optimization and semi-definite optimization, and we use the results as the lower bound of required power of Problem (2).

Remark 5: We note that, even though $p^*_{EH,l}$ is a lower bound of p^*_{EH}, if $\alpha_{\max} \geq \eta\eta_{PA}$, then $p^*_{EH,l} \geq p^*_{BC}$, i.e., the optimal solution in the BC case outperforms the one in the case of energy harvesting with separated antennas. We will provide a brief proof as follows.

Proof: The main idea of the proof is similar to the one in the proof of Theorem 4, i.e., to show that any feasible solution to Problem (10), is also feasible for Problem (3).

Let $(\boldsymbol{p}, \boldsymbol{P}^{\text{t}})$ be a feasible solution to Problem (10). We will show that it is also a feasible solution to Problem (3). It is easy to see that, when $(\boldsymbol{p}, \boldsymbol{P}^{\text{t}})$ satisfies Constraints (2b), (2f), and (10b), it satisfies Constraints (3b), (3d), and (3c), respectively. When the solution satisfies Constraint (2g), it satisfies the first inequality in Constraint (3e). What remains is to show that, when $(\boldsymbol{p}, \boldsymbol{P}^{\text{t}})$ satisfies Constraint (10c), it will satisfy the second inequality of Constraint (3e).

From Constraint (10c), it follows that $P^{\text{t}}_i \leq \eta\eta_{\text{PA}} \sum_{k=1}^{K} p_k |h_{k,i}|^2 - \eta_{\text{PA}} t_{\min} P^{\text{DAC}} < \alpha \sum_{k=1}^{K} p_k |h_{k,i}|^2$, for every i, where the second inequality comes from $\alpha_{\max} \geq \eta\eta_{\text{PA}}$ and $t_{\min}\eta_{\text{PA}} P^{\text{DAC}} > 0$. Thus, Constraint (3c) holds when Constraint (10b) holds.

To summarize, Problem (3) is a relaxation of Problem (10), and the optimum of Problem (3) will be no larger than that of Problem (10). ■

From the proof, we can see that, if $\alpha_{\max} = \eta\eta_{\text{PA}}$ and the power usage of the DAC is ignored, then Problem (10) is equivalent to Problem (3), and thus also equivalent to Problem (1). This means that the importance of considering the power usage of the DAC in HTT can be seen by letting $\eta = \alpha_{\max}/\eta_{\text{PA}}$, and comparing the performance of BC (optimum of Problem (1)) with the performance of HTT (optimum of Problem (10)).

With these results on the performance bounds, we will be able to get a deeper understanding of the two technologies, BC and HTT, through the numerical simulations in the next section.

V. Numerical Study and Results

In this section, we will present the results of four different simulations. For each simulation, the metrics we are interested in are the minimum required power, and the outage probability. An outage occurs when the problem has no feasible solution. For each simulation, the average minimum power was recorded across multiple trials, and for each trial the minimum required power was included only when the problem had a feasible solution (also satisfying the power constraints). One of the goals of the simulations is to compare HTT and BC with respect to these two metrics. In some of the simulations, both the single antenna case and the multiple antenna case were simulated.

TABLE I

Default Simulation Setup

Parameter	Default value		Explanation
	Single antenna	Multiple antennas	
D	$\sim \text{Uniform}(50, 200)$ m		Distance, antenna to primary users
K	1	8	Number of antennas
L	100 m		Side length of the field
M	5		Number of primary users
N	100		Number of secondary users
P	160 W	20 W	Power constraint
P^{DAC}	10^{-3} W		Power of the DAC
R_{p}	1 Mbps		Data rate requirement, primary users
R_{s}	1 Kbps		Data rate requirement, secondary users
T	1		(Normalized) time slot duration
$t_{\min}$	$10^{-5}T$		Minimum transmission time for the transceiver in a timeslot
W	1 MHz		Channel bandwidth
$\alpha_{\max}$	0.5		Maximum backscatter coefficient
η_{PA}	0.625		PA efficiency
σ^2	-80 dBm		Noise power

Miscellaneous parameters	Explanation
$\sim \text{Uniform}(3, 5)$ m	Distance, SU-TX to its SU-RX
$(0, 0)$	Location of antenna, when $K = 1$
$(L\cos(2\pi k/K)/2, L\sin(2\pi k/K)/2)$	Location of k-th antenna, when $K > 1$
$g = 30.6 + 36.7\log_{10}(d)$	Channel gain path-loss model

We will now describe the setting and parameters for the simulations. For reference, the default values of the parameters used in the simulations are summarized in Table I, and are the same across all simulations, unless otherwise stated. Some of the parameters have different values for the single antenna and the multiple antenna cases, indicated by the two columns in the table. When the parameter value is the same for both cases, only one value is given, centered between both columns. In each of the following subsections, a specific subset of the parameters was varied. The parameters that were varied in each subsection are listed in Table II, along with the range of values used in the corresponding simulations.

In the simulations, all the SU-TXs and BS antenna ports are located inside a square field, centered at the origin $(0, 0)$, with side length L (see Fig. 2). By default, $L = 100$ meters. Note that the primary users are not restricted by this field, and *may or may not* be located inside this field. In the single-antenna cases, the base station, together with its antenna, is located at the origin. In the multiple-antenna cases, the DAS base station has $K = 8$ separated antennas, with the k-th antenna located at the point $(L\cos(2\pi k/K)/2, L\sin(2\pi k/K)/2)$.

The power constraint for each antenna in the multiple antenna case is set to $P = 20$ Watts. To compare the energy efficiency between the single antenna and multi-antenna cases, that is the relative benefit of using a distributed antenna setup, we set the power constraint for the single antenna case to

TABLE II
SIMULATIONS AND VARIED PARAMETERS

Varied parameter	Value range	
	Single antenna case	Multi-antenna case
Subsection V.A	Yes	No
D	300 to 500 m	
Subsection V.B	Yes	Yes
L	50 to 200 m	50 to 450 m
Subsection V.C	No	Yes
N		10 to 100

TABLE III
SUMMARY OF SIMULATED CASES

Case	Description
	Harvest-then-transmit (HTT)
HTT Case 1	Uses $\eta = 0.5$
HTT Case 2	Uses $\eta = 0.8$
	Backscatter communication (BC)
Optimal	Sets α_i according to Algorithm 2 (single antenna case) or Algorithm 1 (multiple antenna case)
Greedy	Sets α_i to $\alpha_{\max}$
Over-optimistic	Ignores interference from secondary users

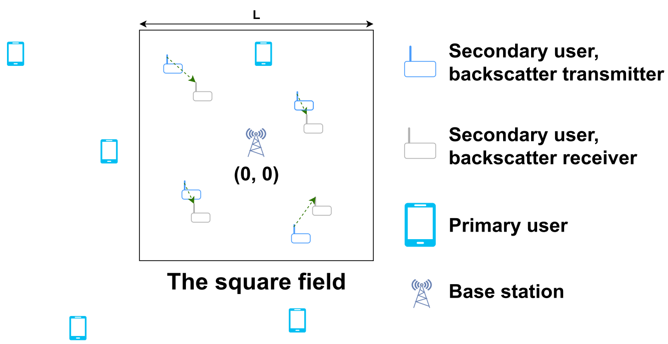

Fig. 2. An illustration of the square field in the single antenna case. All secondary user transmitters are located inside the field, with primary users possibly inside or outside.

$P = 160$ Watts (8 times the power constraint per antenna in the multi-antenna case). This power constraint was chosen only to serve this illustrative purpose, and the primary case of interest in the simulations is the multiple antenna case. For a more in-depth numerical study of the single antenna case using the power constraint $P = 20$ Watts, see [13].

By default, the number of primary users M is 5 and the number of secondary users N is 100. Each primary user was placed randomly and uniformly at a distance (different for each one) between 50 to 200 meters from the origin, which could be either inside or outside the field. The SU-TXs were randomly and uniformly deployed inside the field, while the SU-RXs were located randomly and uniformly 3 to 5 meters away from their corresponding SU-TX.

The channel gains between each pair of devices are based on the path loss model $g = 30.6 + 36.7 \log_{10}(d)$ in dB [36], where d is the distance between the two devices. We should note that this path loss model includes a shadow fading term with standard deviation $\sigma = 4$. The channel bandwidth is 1MHz, and the noise power is -80 dBm. The data rate requirements of the primary users and the SU-RXs are 1Mbps and 1Kbps, respectively. The maximum backscatter coefficient is $\alpha_{\max} = 0.5$. The PA efficiency is $\eta_{\text{PA}} = 0.625$. The power of the DAC, P^{DAC}, is 10^{-3} Watts, and $t_{\min}$ is set to be $10^{-5}T$.

We compare the following cases in the simulations, summarized in Table III. For the backscatter cases, the optimal solution refers to the one obtained by Algorithm 2 when the base station has a single antenna, and the one obtained by Algorithm 1 in the general multiple antenna case. The greedy one corresponds to the greedy backscatter in Remark 3, which sets every backscatter coefficient to its maximum value $\alpha_{\max}$. We also present the results achieved when the interferences from the SU-TXs are ignored, referred to as the over-optimistic case.

For the HTT cases, Case 1 uses the value $\eta = 0.8$, and Case 2 uses $\eta = \alpha_{max} = 0.5$. We should mention that typical RF-DC conversion rates are less than 0.8. Thus, the results for the HTT cases are optimistic in general. In addition, we use the optimum of convex Problem (10) as the lower bound of the required power and the outage probability for the HTT cases for evaluation, as was mentioned in Section IV-D. This means that the results obtained in these simulations may overestimate the performance of the HTT cases. We should mention that the required power in the optimal BC cases is much smaller than the lower bound of the required power for the HTT cases, as will be shown in the following numerical results.

A. Varying the Distance to the Primary Users

In the first simulation, we studied the impact of the distance from the antenna to the primary users on the performance, considering only the single antenna case. In order to better illustrate this effect, the primary users were randomly distributed on the perimeter of a circle centered at the antenna, meaning that the distance was the same for all primary users.

The simulation was performed for distances in the range 300 to 500 m. The results are plotted in Fig. 3a, and Fig. 3b. The solid line with circle marks represents the case where the SU-TXs use BC, and the base station helps them to transmit the data, whereas the dashed line with circle marks represents the case of having no secondary user pairs (i.e., $N = 0$, or only primary users). The green line with diamond marks and the purple one with crosses show the results of HTT Case 1 and Case 2, respectively. The green dashed line is the HTT Case 1 without primary users (only secondary users).

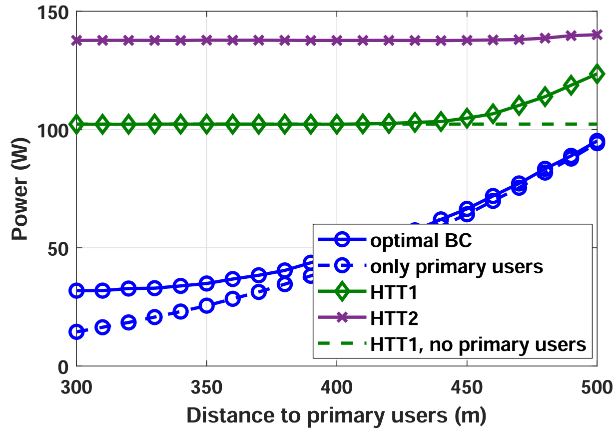

(a)

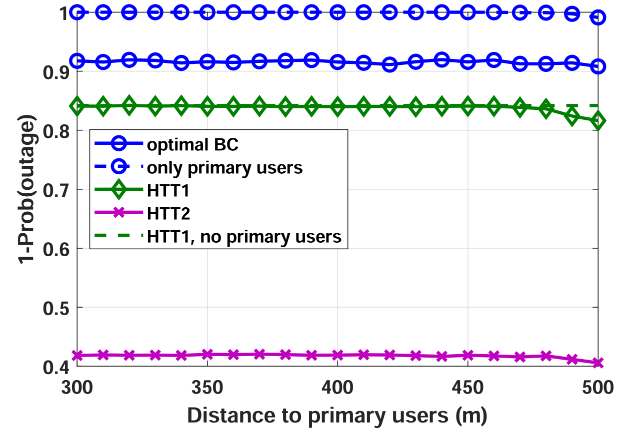

(b)

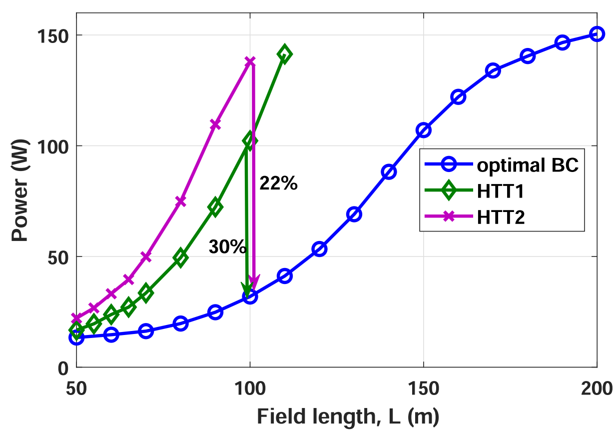

(c)

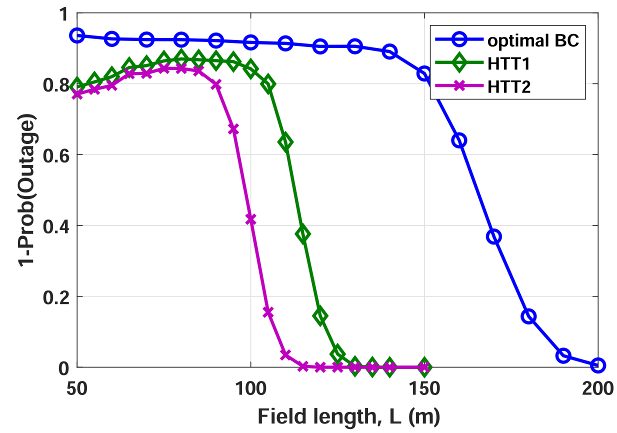

(d)

Fig. 3. Simulation results for the single-antenna base station case. (a) Required power for different distances to the primary users. (b) Outage probability for different distances to the primary users. (c) Required power for different field lengths. (d) Outage probability for different field lengths.

Fig. 3a shows that, as the distance to the primary users increases, the required power when using BC also increases. However, the difference between having secondary users and not having any secondary users diminishes as the distance increases. When using HTT, the required power is much higher than in the BC case. For HTT Case 1, the baseline green dashed line shows that the broadcasting power of the base station required to support 100 SU-TXs to harvest enough power in a field with side length $L = 100$ meters, is still more than the power that is needed to transmit with 1Mbps to the primary users 500 meters away. Thus, the required power of HTT Case 1 with primary users remains almost constant when the distance of the antenna to the primary users is smaller than 440 meters.

In Fig. 3b, we have plotted the probability of being feasible (one minus the outage probability), as a function of the distance from the antenna to the primary users. The labels are the same to the ones in Fig. 3a. For the cases with secondary users, the probability of being feasible stays above 91% when the distance to the primary users is less than 500 meters and the SU-TXs use optimal BC. In the case of HTT1, the probability is about 84%, even without any primary users. The probability achieved by optimal BC is higher than that in the HTT Case 1 and Case 2. We also observe that this probability is not significantly affected by the distance to the primary users, in the range that we considered.

Running 10,000 trials using Algorithm 2 takes about half a minute on a modern commodity laptop. As a comparison, running 4,000 trials using SeDuMi to solve Problem (3) (also in the single-antenna case) takes about 40 minutes on similar hardware. It would therefore be interesting to see if and how the ideas behind Algorithm 2 could be extended to the multiple-antenna case.

B. Varying the Field Length

In the second simulation, we instead varied the side length L of the field, while using the default values for the other parameters. These simulations were performed for both the single antenna, and the multiple antenna case.

Consider first the single antenna case, varying the field length L between 50 and 200 m. We have plotted the required power for the optimal solution in the BC case, the HTT Case 1, and the HTT Case 2, as a function of the field length L in Fig. 3c. The blue curve with circle marks, the green curve with diamond marks, and the purple curve with cross marks, show the required power for the optimal solution in the BC

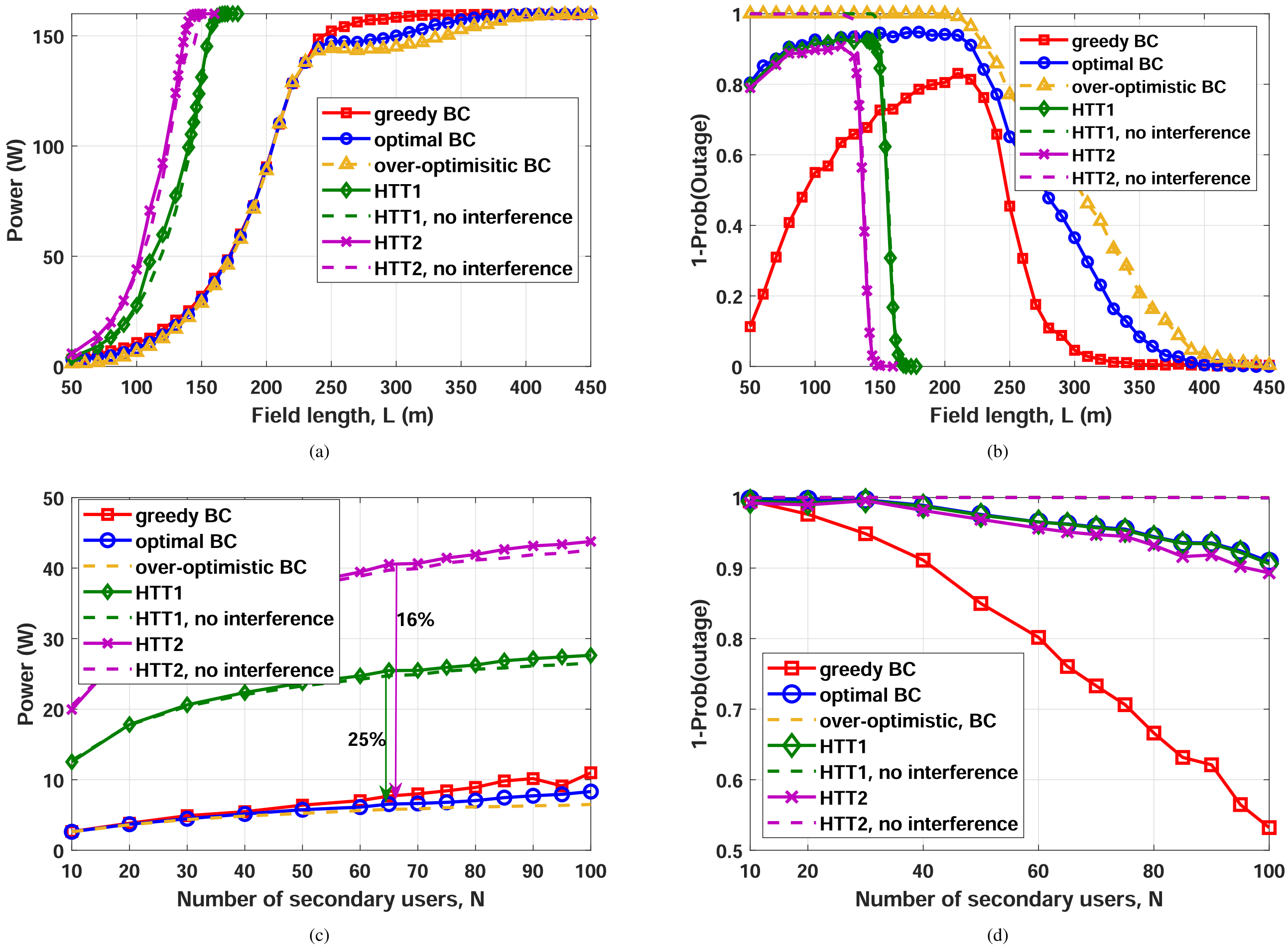

Fig. 4. Simulation results for the multi-antenna base station case. (a) Required power for different field lengths. (b) Outage probability for different field lengths. (c) Required power for different numbers of secondary users. The field length is 100 meters. (d) Outage probability for different numbers of secondary users. The field length is 100 meters.

case, the HTT Case 1, and HTT Case 2, respectively. Fig. 3c shows that, when the field length is 100 m, BC uses 30 % as much power as HTT Case 1, and 22 % as much power as HTT Case 2.

We can see that the required power increases with the field length. The reason is that, as the field length increases, more power is needed to reach the furthest SU-TX to meet its data rate requirement. When we compare the performance of the BC and HTT technologies, we can see that the required power in the BC case is much lower than in the HTT case. At $L =$ 100 meters, the required power for the optimal solution for BC is approximately 31 Watts, which is 70% lower than the required power in the HTT Case 1, and 78% lower than in the HTT Case 2. Recall that the required power in both HTT cases may be greater than what is indicated here, since the plotted results are in fact the lower bound for the power (the solution to Problem (10)).

We then compare the outage probability for the three different cases. We have plotted the probability of being feasible, as a function of L in Fig. 3d, using the same labels. The results show that the data rate requirements of the system are met in more than 50% of the trials when using optimal BC, as long as the field length is less than 160 meters, whereas the problem becomes infeasible for the HTT cases when L is greater than 130 meters. In Fig. 3d, we see that the graphs for both HTT Case 1 and HTT Case 2 have a "bump" between 50 and 100 m. For small field lengths, the distances between secondary users will be very small, causing significant interferences between them. The difference between the BC and HTT graphs is due to the extra power requirement of DAC. The "bump" is caused by a decrease in outage probability as the field length (and the distances between devices) increases and there is less interference, but beyond a certain point, the transmit power of the base station is not high enough to reach the SUs (which causes the sharp drop).

Since the optimal solution in the BC case is much more energy-efficient than in the HTT cases, BC can support larger field sizes than HTT. If we define the maximum feasible field length as the threshold beyond which the outage probability is larger than 99%, then the maximum feasible field length in the BC case is around 200 meters, which is around 54% and 67% greater than the maximum feasible field length in the HTT Case 1 and the HTT Case 2, respectively.

Next, we consider the case with multiple separated antennas, and the results are shown in Fig. 4a. In general, the required power increases with the field length. The required power for the different BC schemes starts to saturate at 160 Watts when the field length is larger than 220 meters, at which point the most problem becomes infeasible. Although the curves of the different BC schemes are close to each other in the figure, the greedy BC scheme requires on average 7% more power than the optimal one. Additionally, the optimal case requires on average 16% more power if the interference is neglected; and in some cases when the field length is small, it requires even twice the power. It shows that the interference should not be neglected when we have massive numbers of backscattering devices or the network is dense.

When we compare the required power of the BC case and the HTT cases, we can observe that the required power of the HTT case increases much faster than the BC case. This shows that BC is much more power-saving than HTT. When we compare the required power for the optimal solution in the BC case where the base station has a single antenna (the result in Fig. 3c), with the case where it has multiple separated antennas (the result in Fig. 4a), we observe that the required power in the multiple-antenna case is much less than in the single-antenna case.

We also check the outage probabilities for the different schemes for different field lengths, as shown in Fig. 4b. The outage probability for the greedy BC is much greater than for the optimal BC case. The gap is noticeably large when the field length is small, that is, when the density of backscattering devices is high. The reason is that the interferences between the secondary devices becomes too large, when they are unable to adjust their backscatter coefficients. In this case, the required transmission power for the base station, to keep the interferences low enough to produce a good SINR, becomes too high. This happens even when the backscatter devices are able to adjust their backscatter coefficients, but the effect is less extreme, which explains why the probability of the BC case being feasible increases as the field length increases from 50 meters to around 200 meters. It is also the reason why the problem is always feasible when backscatter interferences are neglected for the BC case for field lengths less than 200 meters.

The graph for the over-optimistic BC case (yellow graph with triangles), which corresponds to optimal BC but ignoring the interference, shows that the outage probability is approximately 10% to 20% higher when taking into account interference (blue graph with circles, i.e., the optimal BC case). This means that, if we ignore the interference caused by the backscattered signals, then there is an approximately 10% to 20% chance that the BC case is classified as feasible, when it is actually infeasible. When the field length is 350 meters, the greedy scheme almost always results in an infeasible solution (for more than 99% of the cases). The optimal BC scheme extends the feasible field length by 14% to 400 meters.

In summary, given the same number of devices, the network is denser when the field length is smaller, increasing the impact of the interference caused by the backscattered signals, which makes the problems infeasible. When the field length is large, the power that reaches the backscattering devices is low, which becomes the main reason that makes the problem infeasible.

When we compare the performance of BC and HTT, we see that when the field length is small, HTT may have a lower outage probability than the greedy BC scheme. However, it is still worse than the optimal BC scheme. For the cases without considering the interference from the secondary users, the outage probability is almost 0 when the field length is small.

The HTT schemes, no matter whether the interferences by the SU-TXs are considered or not, starts to become infeasible when the field length is greater than 140 meters, as the required power gets closer to the limit. The maximum feasible field length for the HTT case with $\eta = 0.8$ and $\eta = 0.5$ is 168 meters and 148 meters, respectively. Compared to the maximum feasible field length for the HTT cases, the one for the optimal BC case is approximately 1.4 times and 1.7 times greater. This shows that optimal BC can greatly extend the network field size.

When we compare the outage probability for the optimal BC schemes where the base station has a single antenna (the result in Fig. 3d) and multiple separated antennas (the result in Fig. 4b), we observe that the optimal BC in the multiple-antenna case can cover larger field sizes in general. Thus, if we want to support a larger field size, the base station with multiple separated antennas is better than the single antenna case. Therefore, in the following, we focus on the results of the multiple-separated-antenna cases.

C. Varying the Number of Secondary Users

Here, we compare the performances of different schemes as the number of secondary users varies from 10 to 100. The field length L is fixed to 100 meters.

First, we compare the average required power for different schemes and present the result in Fig. 4c. In general, the required power for all schemes increases with the number of secondary users. Since the field length is not too large, the required power is far below the power constraints.

When we compare the performance of the optimal BC scheme with the HTT scheme with $\eta = 0.8$ (in this case $\eta\eta_{\text{PA}} = \alpha_{\max}$), we see that the required power for the BC scheme is on average 20%–30% of the required power for the HTT scheme. Recall the proof of Remark 5. The difference between the optimal solutions to the two problems comes from the DAC power consumption in the HTT scheme. Consequently, we observe that, if the DAC power usage is ignored, the required power for the HTT scheme will be greatly different from reality. While it may be reasonable to ignore the DAC power when the network has very few EH devices and each of them can harvest much more power than the DAC power, the DAC power may not be negligible in massive IoT networks. Thus, the DAC power is an important factor that should be considered in the modelling of the HTT process, especially in massive IoT networks.

When we compare the performance of the optimal BC scheme and the HTT scheme with $\eta = 0.5$, the required power for the BC scheme is on average 12%–15.9% of the required power for the HTT scheme. This shows that BC is much more power-saving than HTT.

We also compare the outage probability for different schemes and present the results in Fig. 4d. The labels are the same as in Fig. 4c. We see that the probability of being feasible for the greedy BC scheme drops very fast as the number of secondary users increases. The failures are due to the strong interferences caused by the backscattered signals, as we have discussed in Section V-B.

We can also see that, when the field length is not too great (recall that it is 100 m in this case), the probability of being feasible for the optimal BC case and the HTT cases are very similar. This is because, at such distances, energy harvesting is still able to supply enough power to the devices for HTT, but note that it requires much more power than using BC. However, when the interferences caused by the secondary users are ignored, the outage probability for both the BC case and the HTT cases is 0, which is up to 10 percentage points higher than when the interferences are taken into account. This shows that the interference caused by the secondary users has greater impact on the required power and whether the problem is feasible or not, for the cases we consider.

D. Summary and Discussion

Based on the numerical results in this section, we can summarize that BC requires much less power than HTT. It can support a field side length almost 1.5 times greater than that of HTT. Furthermore, the interference caused by the backscattered signals should not be neglected when we have massive numbers of backscatter devices and dense networks. We have also observed that the power consumption in DAC and PA should not be neglected in the HTT cases. Otherwise, the result will be greatly inaccurate compared to reality.

BC may still fail when the network is dense due to the strong interference, as we have seen in the simulations. A possible solution to this could be scheduling a subset of secondary users to backscatter simultaneously in a timeslot of the time frame and letting the other secondary users backscatter in the rest of the time frame. Compared to BC, HTT still has some advantages. For example, it can use another channel that has a better channel gain whilst BC can only use the same channel of the carrier emitter. In addition, it is easier to add an energy harvesting circuit to an existing IoT device and reuse or adapt the existing standards and protocols; whilst we probably need to design a new standard and protocol for BC. Although there exist prototypes for BC, it might still take some time before it becomes mature and popular for a broader market.

VI. CONCLUSION

Backscatter communication and energy harvesting can make a wireless network green and sustainable. To gain a deeper understanding of these two technologies and compare their performance, we considered a massive IoT network with multiple primary users and massive IoT devices as secondary users in the paper. We have formulated an optimization problem to minimize the total transmit power of the base station, where the IoT devices use backscatter communication to transmit data to their destinations, and another similar one where the IoT devices use energy-harvest-then-transmit for data transmission.

We proposed numerical algorithms for obtaining the optimal solution for the backscatter communication case. Our theoretical and simulation results show that, in most of the interesting situations, the required transmit power is lower in the backscatter communication case, than in the energy harvesting case. The numerical results also shows the importance of considering the interference from the backscattered signals in modelling, and of considering the power usage in digital-to-analog converters in the energy-harvest-then-transmit process.

For the future work, an interesting research direction would be to generalize our approach to the general multi-user downlink transmission case, where the base station needs to determine the precoding to send different data to different primary users.

APPENDIX

In this section we will prove Theorems 2 and 3, after first proving several intermediate results. Recall that the diagonal elements of the matrix $\mathbf{S}$, given in (4), are strictly positive, and the off-diagonal ones strictly negative. The following lemma will be used to prove Lemma 3 below.

Lemma 1: Consider a square matrix $\mathbf{A}$*, whose diagonal elements are all strictly positive, and off-diagonal ones are all strictly negative. Suppose that the vector* $\boldsymbol{v} > \mathbf{0}$ *satisfies* $\mathbf{A}\boldsymbol{v} \geq \mathbf{1}$ *and* $\mathbf{A}\boldsymbol{v} \neq \mathbf{1}$. *Then there is another vector* $\boldsymbol{w} > 0$ *that satisfies* $\mathbf{A}\boldsymbol{w} > \mathbf{1}$ *and* $0 < w_i \leq v_i$ *for every* $1 \leq i \leq N$, *with strict inequality* $0 < w_k < v_k$ *for some* $1 \leq k \leq N$.

Proof: Let $\boldsymbol{r} = \mathbf{A}\boldsymbol{v}$. Each r_j is strictly increasing as a function of v_j, and strictly decreasing as a function of v_i, for $i \neq j$, since the diagonal elements of $\mathbf{A}$ are all strictly positive, and the off-diagonal elements are all strictly negative.

Since $\boldsymbol{r} \neq \mathbf{1}$, $r_k > 1$ for at least one $1 \leq k \leq N$. Let $\boldsymbol{w}$ be a vector with $w_i = v_i$ for $i \neq k$. By continuity and the above monotonicity property of the elements r_j, there is a real number w_k such that $0 < w_k < v_k$ and $\mathbf{A}\boldsymbol{w} > \mathbf{1}$. ■

The next result will be used to show that an optimal solution to Problem (6) must be unique.

Lemma 2: Consider a square matrix $\mathbf{A}$*, whose diagonal elements are all strictly positive, and off-diagonal ones are all strictly negative. Suppose that there is a positive vector* $\boldsymbol{v} > \mathbf{0}$ *such that* $\mathbf{A}\boldsymbol{v} > \mathbf{0}$. *Then* $\mathbf{A}$ *is invertible.*

Proof: Let $\mathbf{P} = \operatorname{diag}(v_1, \ldots, v_N)$ be the diagonal matrix with entries $v_1, \ldots, v_N$. $\mathbf{P}$ is invertible, since $\boldsymbol{v} > \mathbf{0}$. Consider the matrix $\mathbf{B} = \mathbf{P}^{-1}\mathbf{A}\mathbf{P}$. We will prove that $\mathbf{B}$ is strictly diagonally dominant, and hence invertible, which would then imply that $\mathbf{A}$ is invertible, since they are similar matrices.

Since every element of $\boldsymbol{v}$ is strictly positive, the assumptions on $\mathbf{A}$ imply that the diagonal elements of $\mathbf{B}$ are strictly positive, and the off-diagonal ones are strictly negative. Furthermore, since $\mathbf{A}\boldsymbol{v} > \mathbf{0}$, it follows that $\sum_{j=1}^{N} B_{ij} = \frac{1}{v_i} \sum_{j=1}^{N} A_{ij} v_j > 0$, for every $1 \leq i \leq N$. Therefore

$$|B_{ii}| = B_{ii} > -\sum_{j \neq i} B_{ij} = \sum_{j \neq i} |B_{ij}|,$$

that is, $\mathbf{B}$ is strictly diagonally dominant, and the claim follows. ■

The last of these intermediate results further constrains any optimal solution.

Lemma 3: Any optimal solution $(p^*, \boldsymbol{\alpha}^*)$ *to Problem* (6) *(if one exists) must satisfy* $\mathbf{S}p^*\boldsymbol{\alpha}^* = \mathbf{1}$.

Proof: Suppose that $(p, \boldsymbol{\alpha})$ is an optimal solution to the problem, and let $\boldsymbol{v} = p\boldsymbol{\alpha}$. Since it is a solution to the problem, the constraints imply that $\boldsymbol{v} > \mathbf{0}$ and $\mathbf{S}\boldsymbol{v} \geq \mathbf{1}$. If $\mathbf{S}\boldsymbol{v} = \mathbf{1}$, we are done, so we suppose instead that $\mathbf{S}\boldsymbol{v} \neq \mathbf{1}$. Recall that the diagonal elements of $\mathbf{S}$ are strictly positive, and the off-diagonal ones strictly negative. Therefore, since $\mathbf{S}\boldsymbol{v} \neq \mathbf{1}$, Lemma 1 applies, meaning that there is a vector $\boldsymbol{w} > \mathbf{0}$, satisfying $\mathbf{S}\boldsymbol{w} > \mathbf{1}$, $w_i \leq v_i$ for every $1 \leq i \leq N$, and $w_k < v_k$ for some $1 \leq k \leq N$.

Express the vector $\boldsymbol{w}$ as $\boldsymbol{w} = p\boldsymbol{\alpha}'$. This means that $0 < \alpha'$, since $p > 0$ and $\boldsymbol{w} > 0$. It also means that $\boldsymbol{\alpha}' \leq \boldsymbol{\alpha}$, and $\alpha'_k < \alpha_k$ for some $1 \leq k \leq N$, due to the other properties of $\boldsymbol{w}$. That is, $0 < \boldsymbol{\alpha}' \leq \boldsymbol{\alpha}$. In particular, this means that $B_m(\boldsymbol{\alpha}) < B_m(\boldsymbol{\alpha}')$ for every $1 \leq m \leq M$, since the coefficients b_{mj} in the expression for B_m are all strictly negative for $1 \leq j \leq N$ (see (5)).

Therefore, it holds that both $1 < \mathbf{S}\boldsymbol{w} = \mathbf{S}p\boldsymbol{\alpha}'$, and $1 \leq pB_m(\boldsymbol{\alpha}) < pB_m(\boldsymbol{\alpha}')$, for every $1 \leq m \leq M$. That is, $(p, \boldsymbol{\alpha}')$ is a feasible pair. By continuity, there is an even smaller $0 < p' < p$ satisfying both $1 < \mathbf{S}p'\boldsymbol{\alpha}' < Sp\boldsymbol{\alpha}'$, and $1 < p'B_m(\boldsymbol{\alpha}') < pB_m(\boldsymbol{\alpha}')$ for every $1 \leq m \leq M$. It follows that $(\boldsymbol{\alpha}', p')$ is a feasible solution, which (since $p' < p$) is strictly better than $(\boldsymbol{\alpha}, p)$, contradicting our initial assumption that $(\boldsymbol{\alpha}, p)$ is optimal. Therefore our assumption that $\mathbf{S}\boldsymbol{v} \neq \mathbf{1}$ must be false, and thus $\mathbf{S}\boldsymbol{v} = \mathbf{S}p\boldsymbol{\alpha} = \mathbf{1}$. ∎

Lemma 4: If Problem (6) *is feasible, then it has an optimal solution.*

Proof: Let $\mathcal{F}$ be the feasible set, and suppose that $(\boldsymbol{\alpha}', p')$ is a feasible pair. The subset $\mathcal{F}' = \mathcal{F} \cap \{0 \leq p \leq p'\}$ of pairs that satisfy the constraints in (6), together with the constraint $0 \leq p \leq p'$, is closed and bounded, and therefore compact. Since the objective function is just p, it is smaller on $\mathcal{F}'$ than on the rest of the feasible set $\mathcal{F} \setminus \mathcal{F}'$. Since the objective function is continuous, and $\mathcal{F}'$ is compact, the extreme value theorem implies that the minimum objective value in the feasible set is attained, and consequently that an optimal solution exists. ∎

A. Proof of Theorem 2

Proof: If the problem is feasible, then it must have an optimal solution, by Lemma 4. Consequently, necessity of the condition follows immediately from Lemma 3.

As for sufficiency, suppose that the vector $\boldsymbol{v} > \mathbf{0}$ satisfies $\mathbf{S}\boldsymbol{v} = \mathbf{1}$, and let $(\boldsymbol{\alpha}, p)$ be a pair such that $p\boldsymbol{\alpha} = \boldsymbol{v}$ and $p > 0$. It is always possible to find such a pair that satisfies the constraints of the problem, since p can be as large as possible (recall that Problem (6) ignores the upper power bound P). That is, the problem is feasible. ∎

B. Proof of Theorem 3

Proof: Since we assume that Problem (6) is feasible, Lemma 4 implies that it has an optimal solution $(p, \boldsymbol{\alpha})$. Lemma 3 further implies that this solution must satisfy $\mathbf{S}p\boldsymbol{\alpha} = \mathbf{1}$.

Let $\boldsymbol{v} = p\boldsymbol{\alpha}$, meaning that $\mathbf{S}\boldsymbol{v} = \mathbf{1}$, and let $t = p^{-1} > 0$, so that $\boldsymbol{\alpha} = t\boldsymbol{v}$. Using these new auxiliary variables t and $\boldsymbol{v}$, and recalling that we already have the constraints $t > 0$ and $S\boldsymbol{v} = \mathbf{1}$, the constraints (6b) to (6e) can be reduced to

$$B_m(t\boldsymbol{v}) \geq t > 0, \text{ and} \tag{11}$$

$$\|t\boldsymbol{v}\|_\infty = \|\boldsymbol{\alpha}\|_\infty \leq \alpha_{\max}. \tag{12}$$

Recall that $B_m(t\boldsymbol{v})$ is monotone decreasing as a function of t, and that $B_m(\mathbf{0}) > \mathbf{0}$ (see the paragraph following (5)). Therefore, the constraint (11) is satisfied for every $0 \leq t \leq b_{m0}/(1 - \sum_{i=1}^N b_{mi}v_i)$, where the upper bound is the value of t which achieves equality in (11). Furthermore, the constraint 12 means that $0 < t \leq \alpha_{\max}/\|\boldsymbol{v}\|_\infty$. Therefore, the minimum possible value of $p = t^{-1}$, for which $(\boldsymbol{\alpha}, p)$ is a feasible solution to Problem (6), is attained for the largest possible value of t, which is

$$t = \min\left\{\frac{\alpha_{\max}}{\|\boldsymbol{v}\|_\infty}, \min_{1 \leq m \leq M}\left\{\frac{b_{m0}}{1 - \sum_{i=1}^N b_{mi}v_i}\right\}\right\}.$$

Since the matrix $\mathbf{S}$ and the vector $\boldsymbol{v} > \mathbf{0}$ satisfy the assumptions in Lemma 2, $\mathbf{S}$ is invertible. Therefore, the solution $\boldsymbol{v}$ is unique. Since $\boldsymbol{\alpha} = t\boldsymbol{v}$ and $p = t^{-1}$, the optimal solution $(p^*, \boldsymbol{\alpha}^*)$ is unique and equal to $(t^{-1}, t\boldsymbol{v})$. ∎

References

[1] C. Lundqvist, A. Keranen, B. Smeets, J. Fornehed, C. R. B. Azevedo, and P. vonWrycza, "Ericsson technology review: Key technology choices for optimal massive IoT devices," Ericsson AB, Kista, Stockholm, Tech. Rep., 2018, no. 12. [Online]. Available: https://www.ericsson.com/en/reports-and-papers/ericsson-technology-review/articles/key-technology-choices-for-optimal-massive-iot-devices

[2] S. Bi, Y. Zeng, and R. Zhang, "Wireless powered communication networks: An overview," *IEEE Wireless Commun.*, vol. 23, no. 2, pp. 10–18, Apr. 2016.

[3] G. Yang, C. K. Ho, R. Zhang, and Y. L. Guan, "Throughput optimization for massive MIMO systems powered by wireless energy transfer," *IEEE J. Sel. Areas Commun.*, vol. 33, no. 8, pp. 1640–1650, Aug. 2015.

[4] R. Du, A. Özçelikkale, C. Fischione, and M. Xiao, "Towards immortal wireless sensor networks by optimal energy beamforming and data routing," *IEEE Trans. Wireless Commun.*, vol. 17, no. 8, pp. 5338–5352, Aug. 2018.

[5] Y. Huang, Y. Liu, and G. Y. Li, "Energy efficiency of distributed antenna systems with wireless power transfer," *IEEE J. Sel. Areas Commun.*, vol. 37, no. 1, pp. 89–99, Jan. 2019.

[6] W. Wang *et al.*, "Joint precoding optimization for secure SWIPT in UAV-aided NOMA networks," *IEEE Trans. Commun.*, vol. 68, no. 8, pp. 5028–5040, Aug. 2020.

[7] N. Zhao, Y. Cao, F. R. Yu, Y. Chen, M. Jin, and V. C. M. Leung, "Artificial noise assisted secure interference networks with wireless power transfer," *IEEE Trans. Wireless Commun.*, vol. 67, no. 2, pp. 1087–1098, Feb. 2018.

[8] V. Liu, A. Parks, V. Talla, S. Gollakota, D. Wetherall, and J. R. Smith, "Ambient backscatter: Wireless communication out of thin air," in *Proc. ACM SIGCOMM*, 2013, pp. 39–50.

[9] N. Van Huynh, D. T. Hoang, X. Lu, D. Niyato, P. Wang, and D. I. Kim, "Ambient backscatter communications: A contemporary survey," *IEEE Commun. Surveys Tuts.*, vol. 20, no. 4, pp. 2889–2922, 4th Quart., 2018.

[10] X. Lu, D. Niyato, H. Jiang, D. I. Kim, Y. Xiao, and Z. Han, "Ambient backscatter assisted wireless powered communications," *IEEE Wireless Commun.*, vol. 25, no. 2, pp. 170–177, Apr. 2018.

[11] H. Ju and R. Zhang, "Throughput maximization in wireless powered communication networks," *IEEE Trans. Wireless Commun.*, vol. 13, no. 1, pp. 418–428, Jan. 2014.

[12] S. Bi, C. K. Ho, and R. Zhang, "Wireless powered communication: Opportunities and challenges," *IEEE Commun. Mag.*, vol. 53, no. 4, pp. 117–125, Apr. 2015.

[13] T. O. Timoudas, R. Du, and C. Fischione, "Enabling massive IoT in ambient backscatter communication systems," in *Proc. IEEE Int. Conf. Commun. (ICC)*, Jun. 2020, pp. 1–6.
[14] A. N. Parks, A. Liu, S. Gollakota, and J. R. Smith, "Turbocharging ambient backscatter communication," in *Proc. ACM SIGCOMM*, 2015, pp. 619–630.
[15] G. Wang, F. Gao, R. Fan, and C. Tellambura, "Ambient backscatter communication systems: Detection and performance analysis," *IEEE Trans. Commun.*, vol. 64, no. 11, pp. 4836–4846, Nov. 2016.
[16] G. Vougioukas and A. Bletsas, "Switching frequency techniques for universal ambient backscatter networking," *IEEE J. Sel. Areas Commun.*, vol. 37, no. 3, pp. 464–477, Feb. 2019.
[17] Q. Zhang, H. Guo, Y.-C. Liang, and X. Yuan, "Constellation learning-based signal detection for ambient backscatter communication systems," *IEEE J. Sel. Areas Commun.*, vol. 37, no. 2, pp. 452–463, Feb. 2019.
[18] J. Guo, X. Zhou, S. Durrani, and H. Yanikomeroglu, "Design of non-orthogonal multiple access enhanced backscatter communication," *IEEE Trans. Wireless Commun.*, vol. 17, no. 10, pp. 6837–6852, Oct. 2018.
[19] X. Lu, H. Jiang, D. Niyato, D. I. Kim, and Z. Han, "Wireless-powered device-to-device communications with ambient backscattering: Performance modeling and analysis," *IEEE Trans. Wireless Commun.*, vol. 17, no. 3, pp. 1528–1544, Mar. 2018.
[20] S. Gong, X. Huang, J. Xu, W. Liu, P. Wang, and D. Niyato, "Backscatter relay communications powered by wireless energy beamforming," *IEEE Trans. Commun.*, vol. 66, no. 7, pp. 3187–3200, Jul. 2018.
[21] C. Yang, X. Wang, and K.-W. Chin, "On max-min throughput in backscatter-assisted wirelessly powered IoT," *IEEE Internet Things J.*, vol. 7, no. 1, pp. 137–147, Jan. 2020.
[22] L. Shi, R. Q. Hu, Y. Ye, and H. Zhang, "Modeling and performance analysis for ambient backscattering underlaying cellular networks," *IEEE Trans. Veh. Technol.*, vol. 69, no. 6, pp. 6563–6577, Jun. 2020.
[23] H. Ding, D. B. da Costa, and J. Ge, "Outage analysis for cooperative ambient backscatter systems," *IEEE Wireless Commun. Lett.*, vol. 9, no. 5, pp. 601–605, May 2020.
[24] B. Lyu, Z. Yang, G. Gui, and Y. Feng, "Wireless powered communication networks assisted by backscatter communication," *IEEE Access*, vol. 5, pp. 7254–7262, 2017.
[25] P. Wang, N. Wang, M. Dabaghchian, K. Zeng, and Z. Yan, "Optimal resource allocation for secure multi-user wireless powered backscatter communication with artificial noise," in *Proc. IEEE Conf. Comput. Commun. (INFOCOM)*, Apr. 2019, pp. 460–468.
[26] N.-T. Nguyen *et al.*, "Energy management and time scheduling for heterogeneous IoT wireless-powered backscatter networks," in *Proc. IEEE Int. Conf. Commun. (ICC)*, May 2019, pp. 1–6.
[27] Q. Wu, G. Zhang, D. W. K. Ng, W. Chen, and R. Schober, "Generalized wireless-powered communications: When to activate wireless power transfer?" *IEEE Trans. Veh. Technol.*, vol. 68, no. 8, pp. 8243–8248, Aug. 2019.
[28] G. Yang, D. Yuan, Y.-C. Liang, R. Zhang, and V. C. M. Leung, "Optimal resource allocation in full-duplex ambient backscatter communication networks for wireless-powered IoT," *IEEE Internet Things J.*, vol. 6, no. 2, pp. 2612–2625, Apr. 2019.
[29] R. Du, M. Xiao, and C. Fischione, "Optimal node deployment and energy provision for wirelessly powered sensor networks," *IEEE J. Sel. Areas Commun.*, vol. 37, no. 2, pp. 407–423, Feb. 2019.
[30] A. Wang and C. Sodini, "On the energy efficiency of wireless transceivers," in *Proc. IEEE Int. Conf. Commun.*, Jun. 2006, pp. 3783–3788.
[31] F. A. Potra and S. J. Wright, "Interior-point methods," *J. Comput. Appl. Math.*, vol. 124, nos. 1–2, pp. 281–302, Jan. 2000.
[32] W. Zhao, G. Wang, F. Gao, Y. Zou, and S. Atapattu, "Channel capacity and lower bound for ambient backscatter communication systems," in *Proc. 9th Int. Conf. Wireless Commun. Signal Process. (WCSP)*, Oct. 2017, pp. 1–6.
[33] C. Zhong, X. Chen, Z. Zhang, and G. K. Karagiannidis, "Wireless-powered communications: Performance analysis and optimization," *IEEE Trans. Commun.*, vol. 63, no. 12, pp. 5178–5190, Dec. 2015.
[34] B. Clerckx, R. Zhang, R. Schober, D. W. K. Ng, D. I. Kim, and H. V. Poor, "Fundamentals of wireless information and power transfer: From RF energy harvester models to signal and system designs," *IEEE J. Sel. Areas Commun.*, vol. 37, no. 1, pp. 4–33, Jan. 2019.
[35] J. F. Sturm, "Using SeDuMi 1.02, a MATLAB toolbox for optimization over symmetric cones," *Optim. Methods Softw.*, vol. 11, nos. 1–4, pp. 625–653, 1999.
[36] A. Daeinabi, K. Sandrasegaran, and X. Zhu, "Performance evaluation of cell selection techniques for picocells in LTE-advanced networks," in *Proc. 10th Int. Conf. Electr. Eng./Electron., Comput., Telecommun. Inf. Technol.*, May 2013, pp. 1–6.

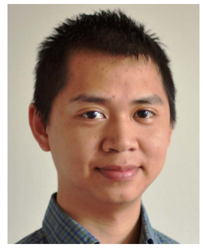

Rong Du received the bachelor's and master's degrees from the Department of Automatic Control, Shanghai Jiao Tong University, in 2011 and 2014, respectively, and the Ph.D. degree in electrical engineering from the School of Electrical Engineering, KTH Royal Institute of Technology, Sweden, in 2018. He worked as a Post-Doctoral Researcher with the Division of Network and Systems Engineering, KTH Royal Institute of Technology. He is currently a Researcher with Ericsson AB, Sweden. His research interests include the IoT, wireless energy transfer, and machine learning.

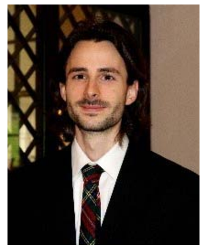

Thomas Ohlson Timoudas (Member, IEEE) received the bachelor's and master's degrees in mathematics from Stockholm University, Sweden, in 2012 and 2013, respectively, and the Ph.D. degree in mathematics from the Department of Mathematics, KTH Royal Institute of Technology, Sweden, in 2019. He is currently a Researcher with the Division of Network and Systems Engineering, KTH Royal Institute of Technology. His research interests include the Internet of Things, machine learning, artificial intelligence, and networked/distributed systems.

Carlo Fischione (Senior Member, IEEE) received the Laurea *(summa cum laude)* degree in electronic engineering and the Ph.D. degree in electrical and information engineering from the University of L'Aquila, Italy, in April 2001 and May 2005, respectively.

He has held research positions at the Massachusetts Institute of Technology, Cambridge, MA, USA, (2015 as a Visiting Professor); Harvard University, Cambridge, MA, USA, (2015 as an Associate Professor); and the University of California at Berkeley, Berkeley, CA, USA, (2004–2005 as a Visiting Scholar and 2007–2008 as a Research Associate). He is currently a Full Professor of Electrical Engineering and Computer Science with the Division of Network and Systems Engineering, KTH Royal Institute of Technology, Stockholm, Sweden. He is also the Director of the KTH Data Science Micro Degree Program, an advanced education program dedicated to Ericsson's researchers worldwide. He has coauthored over 200 publications, including a book, book chapters, international journals and conferences, and international patents. His research interests include applied optimization, wireless, sensor networks, the Internet of Things, and machine learning. He is also an Ordinary Member of DASP (the Italian Academy of History Deputazione Abruzzese di Storia Patria). He received a number of awards, such as the "IEEE Communication Society S. O. Rice" Award for the Best IEEE TRANSACTIONS ON COMMUNICATIONS Paper of 2018, the Best Paper Award of IEEE TRANSACTIONS ON INDUSTRIAL INFORMATICS in 2007, the Best Paper Awards at the IEEE International Conference on Mobile Ad-hoc and Sensor System 2005 and 2009 (IEEE MASS 2005 and IEEE MASS 2009), the Best Paper Award of the IEEE Sweden VT-COM-IT Chapter in 2014, the Best Business Idea Awards from the VentureCup East, Sweden, in 2010, and the Stockholm Innovation and Growth (STING) Life Science in Sweden in 2014, the "Ferdinando Filauro" Award from the University of L'Aquila, in 2003, the "Higher Education" Award from the Abruzzo Region Government, Italy, in 2004, the Junior Research Award from the Swedish Research Council in 2007, and the "Silver Ear of Wheat" Award in History from the Municipality of Tornimparte, Italy, in 2012. He is also the Chair of the IEEE Machine Learning for Communications Emerging Technology Initiative of the IEEE Communication Society. He is also the Editor at Large of IEEE TRANSACTIONS ON COMMUNICATIONS (Machine Learning for Communication and Networking) and an Editor of IEEE JOURNAL ON SELECTED AREAS ON COMMUNICATIONS Series on Machine Learning for Communication and Networking. He has been serving as an Associate Editor for IFAC *Automatica* from 2014 to 2019. Meanwhile, he also has offered his advice as a consultant to numerous technology companies, such as ABB Corporate Research, the Berkeley Wireless Sensor Network Laboratory, Ericsson Research, Synopsys, and the United Technology Research Center. He is also the Co-Founder and the Scientific Director of ELK.